

1 **Intranasal VLP-RBD vaccine adjuvanted with BECC470 confers immunity against**
2 **Delta SARS-CoV-2 challenge in K18-hACE2-mice**

3

4 Katherine S Lee^{1,2}, Nathaniel A Rader^{1,2}, Olivia A Miller², Melissa Cooper², Ting Y Wong^{1,2}, Md.
5 Shahrier Amin³, Mariette Barbier^{1,2}, Justin R Bevere^{1,2}, Robert K Ernst⁴, and F. Heath Damron^{1,2*}

6

7 ¹ Department of Microbiology, Immunology, and Cell Biology, School of Medicine, West Virginia
8 University, Morgantown, WV, USA

9 ² Vaccine Development Center at West Virginia University Health Sciences Center,
10 Morgantown, WV, USA

11 ³Department of Pathology, Anatomy, and Laboratory Medicine, West Virginia University,
12 Morgantown, WV, USA

13 ⁴Department of Microbial Pathogenesis, University of Maryland School of Dentistry, Baltimore,
14 MD, USA

15 * Corresponding Author

16 Corresponding author email address: fdamron@hsc.wvu.edu

17

18

19

20

21

22 **Abstract**

23 As the COVID-19 pandemic transitions to endemic, seasonal boosters are a plausible reality
24 across the globe. We hypothesize that intranasal vaccines can provide better protection against
25 asymptomatic infections and more transmissible variants of SARS-CoV-2. To formulate a
26 protective intranasal vaccine, we utilized a VLP-based platform. Hepatitis B surface antigen-
27 based virus like particles (VLP) linked with receptor binding domain (RBD) antigen were paired
28 with the TLR4-based agonist adjuvant, BECC 470. K18-hACE2 mice were primed and boosted
29 at four-week intervals with either VLP-RBD-BECC or mRNA-1273. Both VLP-RBD-BECC and
30 mRNA-1273 vaccination resulted in production of RBD-specific IgA antibodies in serum. RBD-
31 specific IgA was also detected in the nasal wash and lung supernatants and were highest in
32 VLP-RBD-BECC vaccinated mice. Interestingly, VLP-RBD-BECC vaccinated mice showed
33 slightly lower levels of pre-challenge IgG responses, decreased RBD-ACE2 binding inhibition,
34 and lower neutralizing activity *in vitro* than mRNA-1273 vaccinated mice. Both VLP-RBD-BECC
35 and mRNA-1273 vaccinated mice were protected against challenge with a lethal dose of Delta
36 variant SARS-CoV-2. Both vaccines limited viral replication and viral RNA burden in the lungs of
37 mice. CXCL10 is a biomarker of severe SARS-CoV-2 infection and we observed both vaccines
38 limited expression of serum and lung CXCL10. Strikingly, VLP-RBD-BECC when administered
39 intranasally, limited lung inflammation at early timepoints that mRNA-1273 vaccination did not.
40 VLP-RBD-BECC immunization elicited antibodies that do recognize SARS-CoV-2 Omicron
41 variant. However, VLP-RBD-BECC immunized mice were protected from Omicron challenge
42 with low viral burden. Conversely, mRNA-1273 immunized mice had low to no detectable virus
43 in the lungs at day 2. Together, these data suggest that VLP-based vaccines paired with BECC
44 adjuvant can be used to induce protective mucosal and systemic responses against SARS-
45 CoV-2.

46 **Keywords:** Intranasal vaccine, COVID-19 vaccine, Omicron variant, Delta variant, SARS-CoV-
47 2, K18-hACE2 mice

48 **Introduction**

49 Vaccines prepare the immune system to defend against disease-causing agents through a
50 simulated exposure. Attenuated or inactivated whole-viruses, viral vectors, pathogen proteins,
51 mRNA, and bacterial toxoids, are all used in vaccine formulas administered to hosts to train the
52 immune system to adequately fight off pathogens without an authentic exposure or infection.
53 The immunological memory response that develops from this priming exposure event is
54 oftentimes highly capable of protecting against severe disease and death. Still, the vaccine-
55 elicited immune response differs from a natural response to pathogen exposure and may not
56 always produce superior cellular responses. The intramuscular route of administration is a
57 popular option for vaccine delivery strategies due to its low incidence of site-specific adverse
58 reactions, and optimal immunogenicity for a systemic immune response [1]. Blood supply to the
59 muscles, compared to other tissues, clears adjuvants and other vaccine components more
60 rapidly, leading to the efficient uptake and spread of antigen through the periphery. Circulating
61 antigens are then directed to the lymph nodes where they come into contact with antigen
62 presenting cells (APC) in germinal centers for the generation of antigen-specific T cell and B cell
63 responses [2].

64 Despite the ability of intramuscular vaccines to induce systemic protection against specific
65 pathogens, alternate routes of administration have been investigated to improve comfort and
66 boost the timeframe of protection through elicitation of site-specific immune responses [3,4].
67 Intranasal vaccination is an attractive delivery route for its ability to recapitulate natural infection
68 by respiratory pathogens, priming the mucosa—a site otherwise difficult to generate adaptive
69 immunity in—to provide protection when its needed [5]. There is only one intranasal vaccine
70 currently approved for human use worldwide—FluMist Quadrivalent—although its use is

71 restricted to healthy, non-pregnant individuals between the ages of 2 and 49 due to concerns
72 surrounding its immunogenicity and the use of a live-attenuated virus [6]. With eight orally
73 administered vaccines (the United States have utilized oral vaccines against rotavirus, polio,
74 and others), this together makes a limited number of whole-virus vaccines that directly target the
75 mucosal arm of the immune system [7]. We, and others, hypothesize that a protective mucosal
76 immune response may be the key to ultimate protection against pathogens including SARS-
77 CoV-2 that primarily target and replicate in the upper respiratory tract's mucosal surfaces.

78 Intranasal COVID-19 vaccines are highly desirable as the COVID-19 pandemic evolves and
79 persists [5,8,9]. Not only could they circumvent the discomfort occurring after intramuscular
80 vaccination using the current mRNA-based COVID-19 vaccines, but they may also induce a
81 superior level of protection. In the case of COVID-19 vaccines, studies have shown that
82 vaccinated hosts have relatively weak neutralizing antibody responses against multiple SARS-
83 CoV-2 variants compared to convalescent patients [10]. Specifically, the utilization of
84 intramuscular mRNA vaccines now and into the future as seasonal boosters poses an even
85 bigger problem as it does little to induce mucosal respiratory immunity that is integral to
86 stopping viral replication and therefore preventing high transmission rates among hosts infected
87 with transmissible variants like Omicron. India and China were the first countries to approve the
88 vaccines BBV154 and Ad5-nCoV-S (respectively) for intranasal use [11]. By vaccinating
89 intranasally from the beginning, or by introducing intranasal boosters on top of a completed
90 intramuscular vaccine schedule, the primed immune response against SARS-CoV-2 exposures
91 can evolve to include pathogen specific IgA antibodies as well as greater B cell and tissue-
92 resident memory (T_{RM}) responses throughout the respiratory tract [12–15].

93 Previously, our lab developed the experimental BReC-CoV-2 vaccine that was effective against
94 SARS-CoV-2 challenge in K18-hACE2-transgenic mice when two doses were administered
95 either first intramuscularly (prime) then intranasally (boost), or both intranasally [16]. To build

96 upon the protection of this formulation when administered intranasally, we aimed to improve the
97 overall immunogenicity by utilizing a virus-like particle (VLP) antigen containing SARS-CoV-2
98 WA-1 Receptor Binding Domain (RBD) proteins conjugated using the SpyTag system to a
99 Hepatitis B surface antigen (HbsAg) [17]. The VLP-RBD particle increases the ratio of RBD
100 antigen in the vaccine formulation compared to the RBD-CRM used in BReC-CoV-2. Similar to
101 BReC-CoV-2, this VLP-based vaccine was then adjuvanted with the TLR4-agonist Bacterial
102 Enzymatic Combinatorial Chemistry 470 (BECC 470) to enhance both the cellular and humoral
103 immune responses [18,19]. Intranasal administration of two doses of the VLP-RBD-BECC
104 vaccine to K18-hACE2 mice provided equal protection against disease manifestation and
105 morbidity, as compared to two intramuscular administrations of an mRNA vaccine (mRNA-1273;
106 1/10th human dose) after intranasal challenge with a lethal dose of the SARS-CoV-2 Delta
107 variant. VLP-RBD-BECC limited viral replication in the upper airway at two days post-challenge
108 and maintained a reduction in viral RNA in the nasal wash, lung, and brain, between days two
109 and 10. VLP-RBD-BECC vaccinated mice showed similar serum IgG titers to mRNA vaccinated
110 mice. Importantly, intranasal VLP-RBD-BECC elicited greater RBD specific IgA antibody levels
111 in the lung and nasal cavity than mRNA vaccination or challenge alone. Compared to mRNA,
112 VLP-RBD-BECC consistently maintained low histopathological inflammation scores and
113 concentrations of proinflammatory CXCL10 in the lung tissue as well. VLP-RBD-BECC elicited
114 reduced amounts of Omicron-specific antibodies, however, two doses of the vaccine still
115 demonstrated some protection against viral replication in the lungs of mice following challenge
116 with the Omicron variant.

117 **Methods**

118 ***Ethics and Biosafety Statement***

119 B6.Cg-Tg(K18-ACE2)2PrImn/J transgenic mice were purchased from Jackson Laboratories and
120 used for vaccination and viral challenge studies under West Virginia University IACUC protocol

121 #2009036460. Mice were continuously monitored for adverse reactions to vaccination and for
122 morbidity after challenge and were humanely euthanized according to our lab's disease scoring
123 system. West Virginia University's Biosafety Level 3 Laboratory was used for SARS-CoV-2
124 challenge studies under IBC protocol #20-09-03. Before additional analysis in BSL2 laboratory
125 space, all mouse tissues obtained from BSL3 were treated with 1% Triton by volume or placed
126 in TRIzol (Zymo R2050-1) to inactivate virus.

127 ***Formulation of VLP-RBD-BECC vaccine and K18-hACE2 mouse vaccination***

128 SARS-CoV-2 Wu RBD proteins were cloned into and purified from *Komgataella phaffi* as
129 previously described [20–22]. To form the VLP, RBD-SpyTag antigens were incubated overnight
130 with HBsAg-SpyCatcher VLP [23,24]. The BECC 470 adjuvant was obtained from Dr. Robert
131 Ernst at the University of Maryland [18]. Vaccines were prepared in batch by sonicating 25µg
132 BECC 470 per dose in water for 15min, then adding RBD-HBsAg VLP (10µg per dose) and
133 incubated rotating at room temperature for 2hrs. Before administration, 10X PBS was added to
134 bring the dose volume to 50µL. Female 7-week-old K18-hACE2 mice were intranasally
135 vaccinated with 25µL per nare under anesthesia with intraperitoneal ketamine (Patterson
136 Veterinary 07-803-6637)/xylazine (Patterson Veterinary 07-808-1947). No-vaccine no-challenge
137 control mice were administered 50µL 1X PBS intramuscular in the hind flank. mRNA control
138 mice were administered 50µL mRNA-1273 vaccine intramuscular in the hind flank as well. All
139 vaccine groups received a second identical dose 4 weeks later.

140 ***Quantification of anti-SARS-CoV-2 RBD IgG antibodies by ELISA***

141 Submandibular bleeds to collect serum were performed to assess immunogenicity 4 weeks after
142 prime and boost doses. Serum was also collected at euthanasia via cardiac puncture. Anti-
143 SARS-CoV-2 RBD IgG levels were quantified using ELISA and a method described previously
144 [25]. High binding plates were coated overnight with 2 µg/mL RBD. The next day, plates were

145 washed 3x and blocked with 3% nonfat milk in PBS-Tween20. After an hour incubation at room
146 temperature, plates were washed 3x then prepared for sample: 5 μ L of serum in 95 μ L 1%
147 nonfat milk-PBS-Tween20 was added to the top row, and 50 μ L of 1% nonfat milk-PBS-
148 Tween20 was added to the remaining wells for dilution across two plates. Samples were diluted
149 1:2 from row A of plate 1 to row G of plate 2, discarding before dilution into row H. Samples
150 incubated shaking at room temperature for 1 hr. Plates were washed 4x before adding 100 μ L
151 secondary antibody (goat anti-mouse IgG HRP; Novus Biologicals NB7539) (diluted 1:2000) in
152 1% nonfat milk-PBS-Tween20 to all wells and shaking for an additional 1 hr at room
153 temperature. Non-bound antibodies were washed with 5x washes and 100 μ L TMB substrate
154 was added to all wells. After 15 min incubation in the dark, 25 μ L 2N sulfuric acid was added to
155 stop development and plate absorbances were read at 450 nm on the Synergy H1 plate reader.
156 Serum antibody levels were quantified using Area Under the Curve analysis in GraphPad Prism
157 V9.0.0.

158 ***Quantification of anti-SARS-CoV-2 RBD IgG antibodies by ELISA***

159 To measure anti-RBD IgA in K18-hACE2 mouse tissues following challenge, the ELISA protocol
160 described previously was utilized with minor adaptations. High-binding 96-well plates were
161 coated with RBD, washed and blocked following the same protocol as was used to measure
162 IgG. Mouse samples were added to the top row of wells (5 μ L of serum in 95 μ L 1% nonfat milk-
163 PBS-Tween20; 20 μ L lung supernatant in 80 μ L 1% nonfat milk-PBS-Tween20; 100 μ L nasal
164 wash), then diluted down the columns 1:2 discarding before the last well. After 2 hours of
165 incubation shaking at room temperature, 100 μ L anti-IgA secondary antibody diluted 1:10000
166 (goat anti-mouse IgA HRP; Novus Biologicals NB7504) was added to all wells. Secondary
167 antibody was left to incubate for 2 hours, then plates were washed, developed, and read as
168 previously described.

169 ***In vitro SARS-CoV-2 RBD ACE2 binding assay***

170 Neutralizing potential of serum antibodies collected from vaccinated K18-hACE2 mice pre- and
171 post-challenge was analyzed using MSD's V-PLEX SARS-CoV-2 Panel 22 Mouse IgG kit
172 (K15563U-2). Binding to the following antigens was assessed: COV-2 RBD, Delta RBD,
173 Gamma RBD, Beta RBD, Alpha RBD, and Omicron RBD. Serum from mice euthanized at 10
174 days post- challenge or from 4-week post-boost submandibular bleeds was diluted at 1:5, 1:50,
175 1:500, and 1:5000 and analyzed following the manufacturer's protocol. Binding (%
176 neutralization) was measured via electrochemiluminescence values compared to baseline wells
177 with no antibody binding. The percent neutralization 50 (PRNT50) was calculated by fitting a
178 nonlinear regression curve to the plotted percent binding values and interpolating unknowns in
179 GraphPad Prism version 9.

180 ***In vitro authentic SARS-CoV-2 plaque reduction assay***

181 Vero E6 ACE2/TMPRSS2 cells were plated at 70,000 cells per well in 24-well plates and
182 incubated at 37°C and 5% CO₂ for 24 hours. Stock SARS-CoV-2 Delta virus (B.1.617.2 hCoV-
183 19/USA/WV- WVU-WV118685/2021) was diluted in supplemented DMEM media. Mouse serum
184 was diluted 1:5 then ten-fold serial dilutions in media. Diluted mouse serum was mixed with
185 diluted virus in a 1:1 (v/v) ratio and incubated at room temperature for 30 minutes. Cell media
186 was aspirated. 100µl of sample (serum + virus) was added to each well. Plates were incubated
187 at 37°C and 5% CO₂ for 1 hour. Plates were gently rocked by hand every 15 minutes. After
188 incubation, 1 mL of 0.6% carboxymethylcellulose overlay was added to each well. Plates were
189 incubated at 37°C and 5% CO₂ for 4 days. On day 4, the overlay was aspirated. Wells were
190 fixed with 10% neutral-buffered formalin and stained with 0.1% crystal violet before plaques
191 were counted. Cell culture and plaque assay reagent recipes were adapted from Case, et al
192 [26].

193 ***SARS-CoV-2 challenge of K18-hACE2 mice***

194 Stocks of the SARS-CoV-2 Delta variant B.1.617.2 hCoV-19/USA/WV- WVU-WV118685/2021
195 (GISAID Accession ID: EPI_ISL_1742834) were created from a patient sample at WVU that was
196 propagated in Vero E6 cells (ATCC-CRL-1586) [27]. The stocks were sequenced to confirm
197 there were no mutations. Omicron variant (strain BA.5) stocks were obtained from the labs of
198 Dr. Luis Martinez-Sobrido and Dr. Jordi Torrelles at the Texas Biomedical Research Institute. At
199 the time of challenge, vaccinated and control K18-hACE2 mice were anesthetized with an IP
200 injection of ketamine/xylazine, then 25 μ L of a 10^4 PFU solution of Delta or 10^5 PFU solution of
201 Omicron virus was administered by pipette into each nare (50 μ L total dose).

202 ***Disease scoring of SARS-CoV-2 challenged mice***

203 K18-hACE2 mice were evaluated every day after challenge to track disease progression
204 through in-person health checks and using the SwifTAG video monitoring system. Rectal
205 temperatures and weight measurements were recorded each day in addition to scores related to
206 weight loss, changes in activity, appearance, eye closure/conjunctivitis, and respiration. Scores
207 were awarded based on severity of disease phenotypes and follow a scale that has been
208 described previously [17,25,27,28]. On each day, scores in each category were combined and
209 recorded as one overall numerical score. Mice that received a total score of 5 or reached 20%
210 weight loss before day 10 post-challenge were humanely euthanized.

211 ***Mouse euthanasia and tissue collection***

212 At day 2, 10, or due to meeting humane endpoint criteria, K18-hACE2 mice were euthanized
213 with IP pentobarbital (390mg/kg) (Patterson Veterinary 07-805-9296) followed by cardiac
214 puncture. Blood from cardiac puncture was centrifuged to collect the serum for downstream
215 analysis. Lung and brain tissue were dissected out for downstream histology, serology, and
216 quantification of viral burden. Homogenization of lung and brain was performed following a
217 previously established protocol [17,25]. A nasal wash was performed on each mouse by

218 pushing PBS (1mL) by catheter through the nasal pharynx and collected for analysis. For RNA
219 purification in BSL2, lung and brain homogenate as well as nasal wash was treated with TRIzol
220 Reagent.

221 ***SARS-CoV-2 plaque assay from tissue homogenate***

222 Vero E6 ACE2/TMPRSS2 cells were plated at 150,000 cells per well in 12-well plates and
223 incubated at 37°C and 5% CO₂ for 24 hours. Mouse lungs collected at euthanasia were
224 weighed then homogenized in 1mL PBS. Then, homogenate was centrifuged at 15,000 x g for 5
225 minutes. Supernatant from mouse lung homogenate was diluted in media 1:3, 1:10, then four
226 ten-fold serial dilutions. Cell media was aspirated. 200µl of sample was added to each well, in
227 duplicate. Plates were incubated at 37°C and 5% CO₂ for 1 hour. Plates were gently rocked by
228 hand every 15 minutes. After incubation, 2 mL of 0.6% carboxymethylcellulose overlay was
229 added to each well. Plates were incubated at 37°C and 5% CO₂ for 4 days. On day 4, the
230 overlay was aspirated. Wells were fixed with 10% neutral-buffered formalin and stained with
231 0.1% crystal violet.

232 ***qRT-PCR quantification of SARS-CoV-2 viral copy number in mouse tissues***

233 RNA from nasal wash, lung, and brain homogenates of virus-challenged mice was purified using
234 the the Direct-zol RNA miniprep kit (Zymo Research R2053) according to the manufacturer's
235 protocol. qPCR of the SARS-CoV-2 nucleocapsid gene was then performed for each mouse
236 and sample using the Applied Biosystems TaqMan RNA to CT One Step Kit (ThermoFisher
237 Scientific 4392938) to measure viral copy number via transcript number with specifications for
238 each reaction that have been described previously [17,25,27,28].

239 ***Measurement of CXCL10 concentrations in mouse serum and lung***

240 Concentrations of CXCL10 in K18-hACE2 mice were measured in serum and lung supernatant
241 collected at euthanasia using the Mouse Magnetic Luminex Assay kit for mouse CXCL10/IP-

242 10/CRG2 (R&D Systems LXSAMSM-01). Both serum and supernatant samples were diluted 1:2
243 in the kit's Calibrator Diluent RD6-52 then utilized in the assay procedure provided by the
244 manufacturer. The assay plate was read on the Luminex MAGPIX instrument and chemokine
245 levels were quantified based on a standard curve.

246 ***Histopathological evaluation of lung tissue inflammation***

247 The left lobes of mouse lungs were collected at euthanasia and stored in 10% neutral buffered
248 formalin for one week to fix. Fixed tissues were sectioned and mounted on slides, then
249 Hematoxylin and Eosin stained for analysis. Primary histopathological scoring was performed by
250 iHisto under the supervision of chief pathologist Michelle X. Yang, MD, PhD. H&E-stained slides
251 were evaluated for acute and chronic inflammation. Acute inflammation was marked by the
252 infiltration of neutrophils in the parenchyma, blood vessels, and airways. Chronic inflammation
253 was marked by mononuclear infiltrates in the same areas of the tissue. Semiquantitative scores
254 for each condition (0- none, 1- minimal, 2- mild, 3- moderate, 4- marked, 5- severe) were
255 awarded for tissue from each mouse. Additional analysis was performed by West Virginia
256 University's Department of Pathology to identify more finite characteristics of inflammatory
257 pathology. Margination of inflammatory cells in blood vessels was evaluated and graded as
258 none, mild, moderate or severe. Viral cytopathic changes in the epithelial and interstitium were
259 also evaluated and graded as absent, mild, moderate or severe. Other parameters that were
260 evaluated included type of inflammatory cells, distribution of the inflammatory aggregates,
261 presence of pneumonic infiltrates, bronchiolitis and vasculitis.

262 ***Statistical analyses***

263 The statistical analysis of data sets in this study was performed using GraphPad Prism version
264 9. Mouse experiments were performed with an n=10 for all groups, with n=3 mice per group
265 euthanized on day 2 and n=7 mice euthanized at day 10 post-challenge. Normally distributed

266 data sets were compared using ordinary one-way ANOVA with Tukey's multiple comparisons
267 tests. Kaplan-Meier survival curves were created to compare the survival of vaccinated K18-
268 hACE2 mice following viral challenge. Unpaired t-tests were utilized to compare two data sets.

269 **Results**

270 **VLP-RBD adjuvanted with BECC 470 (TLR4 agonist) induces IgG and IgA antibody** 271 **production when administered via the nasal route**

272 SARS-CoV-2 infection induces mucosal immune responses including production of IgA
273 antibodies. To assess mucosal responses as well as systemic antibodies elicited by our novel
274 VLP-RBD-BECC vaccine, K18-hACE2 transgenic mice were primed via the intranasal (IN) route
275 using 10 µg VLP-RBD formulated with 25 µg BECC 470 (Fig. 1A). A control group of mice were
276 vaccinated via the intramuscular (IM) route with 1/10th of a human dose (10 µg) of mRNA-1273--
277 a highly protective Spike protein-based COVID-19 vaccine that has been used to vaccinate a
278 large portion of the United States population. After four weeks, mice were administered a
279 second identical boost dose of either vaccine to mimic the human COVID-19 vaccine schedule.
280 We measured levels of IgG specific to the SARS-CoV-2 Spike protein receptor binding domain
281 (RBD) at four weeks post-prime (Fig.1B), four weeks post-boost (Fig. 1C), and after challenge
282 with the SARS-CoV-2 Delta strain (Fig. 1D). IM mRNA-1273 vaccinated mice showed high IgG
283 levels post-prime whereas IN VLP-RBD-BECC mice showed relatively low early antibody
284 responses. However, at post-boost the antibody levels in IN mice rose to levels near IM mRNA,
285 albeit still significantly lower (Fig. 1C). At 10 days post-challenge with Delta, RBD specific IgG
286 levels from IN VLP-RBD-BECC or mRNA remained similar to post-boost (no significance) (Fig.
287 1D). mRNA vaccines are known to induce low levels of IgA in serum [29,30]; however, it is not
288 clear if mRNA induces mucosal antibodies in mice. At 10 days post-challenge, low RBD-specific
289 IgA levels were indeed detectable in the serum of IM mRNA vaccinated mice (Fig. 1E).
290 vaccination with IN VLP-RBD-BECC, however, induced anti-RBD IgA antibodies at a much

291 greater level in serum (Fig.1E), nasal wash (Fig. 1F) and lung supernatants (Fig. 1G) post-
292 challenge. These data confirm that intranasal vaccination with VLP-RBD-BECC can induce
293 RBD-specific IgG antibodies in addition to highly desirable IgA antibodies.

294 **IN VLP-RBD-BECC vaccinated K18-hACE2 mice produce broadly neutralizing antibodies**
295 **against SARS-CoV-2 variants**

296 One tenet of highly effective antibody responses is pathogen neutralization which blocks host
297 cell receptor binding for viral entry. Antibodies raised in response to natural infection or
298 vaccination bind the SARS-CoV-2 spike protein to block host cell ACE2 receptor binding and
299 thus inhibit downstream viral replication and the progression of infection. To assess whether or
300 not anti-RBD IgG antibodies from IN VLP-RBD-BECC could execute this inhibition, we
301 performed an *in vitro* ACE2-RBD binding inhibition assay using the serum from vaccinated K18-
302 hACE2 at euthanasia post-challenge. Serum IgG antibodies from IM mRNA vaccinated mice
303 bound RBD from the ancestral, Alpha, Beta, and Delta SARS-CoV-2 variants of concern (VOC)
304 and inhibited ACE2 binding at a greater capacity than serum from IN VLP-RBD-BECC mice *in*
305 *vitro* (Fig. 2A). VLP-RBD-BECC antibodies at a 1:500 dilution still inhibited greater than 50%
306 ACE2 binding to all VOC (Fig. 2A). At the greatest dilution, 1:5000, serum from both vaccinated
307 groups dropped below 50% binding inhibition. It should be noted that mRNA immunized mice
308 have the highest concentration of RBD-binding antibodies in serum post-vaccination and
309 challenge (Fig. 1). IgG antibodies from VLP-RBD-BECC showed a calculated percent binding
310 PRNT50 of 2341 against Delta RBD which was not dramatically reduced compared to the
311 PRNT50 of mRNA-elicited antibodies at 3741 (Fig.2B). Authentic virus neutralization was further
312 evaluated in a viral plaque reduction assay where the SARS-CoV-2 Delta variant was
313 propagated *in vitro* with decreasing concentrations of serum from vaccinated mice collected
314 post-boost. At a low dilution (1:10), mRNA vaccinated mouse serum fully prevented plaque
315 formation (100% reduction) and at higher dilutions (1:100 and 1:1000) still reduced plaque

316 formation by 88% or more (Fig. 3). Serum from VLP-RBD-BECC vaccinated mice was also
317 highly effective at neutralizing virus to prevent plaque formation when added to culture media at
318 a 1:10 dilution and reduced more than 88% or 78% of plaques at higher dilutions (1:100 and
319 1:1000 respectively). These assays show that although IgG antibodies elicited by our VLP-RBD-
320 BECC vaccine have reduced inhibitory activity compared to those from mRNA, total antibodies
321 (which may include IgM, IgA and other antibody subclasses) from these mice are still highly
322 effective at limiting SARS-CoV-2 viral replication and plaque formation *in vitro*.

323 **IN VLP-RBD-BECC protects mice against challenge with SARS-CoV-2 Delta variant**

324 Each major SARS-CoV-2 VOC to emerge after the ancestral Wuhan strain, has presented
325 pathological differences in the K18-hACE2 challenge model [27,31–33]. In particular, we have
326 observed that the Delta variant requires a slightly higher dose to cause 100% mortality, but also
327 that the tissue inflammation signatures and immunological response in mice are significantly
328 different than other variants [27]. We challenged the IN VLP-RBD-BECC and IM mRNA-1273
329 vaccinated K18-hACE2 mice to evaluate protection conferred against the Delta variant. Four
330 weeks after boosting, mice were intranasally challenged them with a lethal dose (10^4 PFU) of
331 the SARS-COV-2 Delta variant to measure protection (Fig. 1A). Intranasal and intramuscular
332 vaccines were equally matched in their disease-limiting abilities (Fig. 4). Compared to PBS-
333 vaccinated and challenged mice, IM mRNA and IN VLP-RBD-BECC vaccinated mice
334 maintained low disease scores over the course of the 10-day challenge window (Fig. 4A). IN
335 VLP-RBD-BECC mice did not experience dramatic weight loss or drops in temperature, similar
336 to the IM mRNA group (Fig. 4BC). VLP-RBD-BECC also conferred 100% survival compared to
337 non-vaccinated mice which reached total morbidity and required humane euthanasia by day 6
338 post-challenge (Fig. 4D). This data together suggests that VLP-RBD-BECC administered by two
339 intranasal doses is as effective as mRNA-1273 at conferring protection against morbidity and
340 mortality in SARS-CoV-2 related disease in K18-hACE2-mice.

341 **SARS-CoV-2 viral replication is limited by intranasal VLP-RBD-BECC**

342 In our challenge study, VLP-RBD-BECC and mRNA vaccinated K18-hACE2 mice were
343 euthanized at day 2 and day 10 post-Delta challenge to assess the vaccines' ability to limit viral
344 replication. Authentic plaque assays using lung supernatant from the mice euthanized at day 2
345 showed that IN VLP-RBD-BECC vaccination and IM mRNA significantly limited viral replication
346 in the lung compared to the PBS-vaccination control (Fig. 5A). Additional qRT-PCR analyses of
347 the mice's nasal wash, lung and brain tissues further supported this finding. SARS-CoV-2 viral
348 nucleocapsid RNA copies were significantly lower in the nasal wash of VLP-RBD-BECC mice
349 compared to PBS vaccinated mice at day 2 and was further reduced at day 10 (Fig. 5B). In the
350 lung, viral RNA burden was significantly lower in mRNA vaccinated mice than the PBS group,
351 however there was no significant reduction in the viral RNA burden of VLP-RBD-BECC lungs at
352 day 2 (Fig. 5C). At day 10, viral RNA burden in the lungs in both vaccine groups had reduced
353 significantly from the level of controls, although it remained slightly above the limit of detection
354 (Fig. 5C). Both vaccines prevented dissemination to and detection of viral RNA in the brain at 10
355 days post-challenge when it was detectable in the brain tissue of control mice (Fig. 5D).

356 **Intranasal vaccination limits the production of CXCL10 following SARS-CoV-2 challenge**
357 **in K18-hACE2 mice**

358 CXCL10 is a potent mediator of inflammation and immune cell homing to the tissues during
359 SARS-CoV-2 infection [34]. It's production in the lung is linked to the cytokine storm
360 experienced by hospitalized patients with severe cases of COVID-19 [35]. Previously, we
361 identified that K18-hACE2 mice have high concentrations of CXCL10 in the lung 6 days post
362 delta variant challenge [27]. To assess if vaccination strategies to protect individuals against
363 severe COVID-19, including VLP-RBD-BECC, confer protection in part by limiting the production
364 of the chemokine, we quantified CXCL10 levels in the serum and lung supernatant of
365 vaccinated mice after Delta SARS-CoV-2 challenge. In the serum, CXCL10 production

366 increased at day 2 after viral challenge in PBS vaccinated control mice (Fig.6A). By day 10, this
367 concentration had reduced slightly but at both timepoints, the concentration of the chemokine in
368 IM mRNA or IN VLP-RBD-BECC remained low. CXCL10 production also peaked in the lung
369 tissue of PBS vaccinated mice at day 2, to much higher concentrations than were detected in
370 the serum (Fig.6B). In vaccinated mice, CXCL10 concentrations in the lung were also limited
371 with no significant change between timepoints. The lack of CXCL10 production seen in the
372 serum and lungs of vaccinated mice when compared to controls, demonstrate that vaccination
373 effectively limits the production of proinflammatory chemokines produced in response to viral
374 challenge.

375 **Intranasal VLP-RBD-BECC vaccination ameliorates lung inflammation in K18-hACE2**
376 **mice after Delta challenge**

377 As a final aspect of vaccine evaluation, lung inflammation was measured by histopathological
378 scoring of acute and chronic inflammation phenotypes. No significant inflammation was seen in
379 the lungs of mice in the control group which served as a comparison to vaccine groups (Fig.
380 67A). Delta challenge in PBS-vaccinated mice lead to viral cytopathic and reactive-proliferative
381 changes in the epithelia of the terminal bronchioles, alveoli, and interstitial cells. Marked
382 margination of inflammatory cells in blood vessels was observed and associated with a diffuse
383 lymphocyte and histiocyte rich inflammatory infiltrate that involved 50-75% of the pulmonary
384 parenchyma. At 2 days post-challenge, intramuscularly vaccinated mice showed higher acute
385 inflammation scores than the intranasal group, suggesting that our intranasal vaccine better
386 protects mice from early development of lung infection than IM mRNA, perhaps due to the route
387 of administration and localized immune responses (Fig.7B). Interestingly, PBS vaccinated mice
388 showed much lower lung inflammation at this time point than IM mRNA mice (there was no
389 significant difference between PBS and IN VLP-RBD-BECC), suggesting perhaps a delayed
390 inflammatory response to virus in the tissue. IM mRNA vaccinated mice euthanized 10 days

391 post-challenge were given low scores for acute inflammation which were not statistically
392 different from IN VLP-RBD-BECC mice (Fig.7C). The diminished extent of pulmonary
393 involvement was further supported by the observation of no significant margination of
394 inflammatory cells or viral cytopathic changes in the vaccinated groups which decreased by day
395 10 (Fig.7D). Overall, mice that were vaccinated either with IM mRNA or IN VLP-RBD-BECC
396 showed marked attenuation of total inflammation compared to PBS vaccination, and involved
397 less than 25% of the parenchyma. Inflammation in vaccinated mice consisted predominantly of
398 tight, peribronchial and perivascular lymphocyte-rich aggregates (Fig.7EF). In total this
399 histopathological analysis shows that IN VLP-RBD-BECC is able to control lung inflammation in
400 the lungs of mice throughout the post-challenge window against SARS-CoV-2 related lung
401 inflammation.

402 **Mice are less protected by intranasal VLP-RBD-BECC against Omicron challenge**

403 The rise of the SARS-CoV-2 Omicron variant to clinical dominance resulted in a reduction of the
404 protection that vaccines formulated against ancestral strains of the virus could provide. Using
405 serum collected at euthanasia from IN VLP-RBD-BECC mice challenged with the Delta variant,
406 we measured the capacity of IgG antibodies to bind Omicron RBD and thus prevent ACE2
407 binding. VLP-RBD-BECC -elicited antibodies showed reduced RBD binding against the variant
408 at dilutions of 1:5 and 1:50 compared to antibodies from mRNA-vaccinated mice (Fig.8A). To
409 determine how this reduced neutralization activity correlated to a potential reduction in
410 protection against the SARS-CoV-2 Omicron virus, we vaccinated a new cohort of mice with two
411 doses of mRNA intramuscularly, or VLP-RBD-BECC intranasally. After prime, VLP-RBD-BECC
412 mice again showed lower amounts of anti-Wuhan RBD IgG antibodies in serum, which
413 increased post-boost (Fig.8B). The utility of matching vaccines to viral variant has been argued
414 as a superior method of providing protection, resulting in the formulation of bivalent (multi-
415 variant) mRNA vaccines for COVID-19 [36,37]. We repeated antibody quantification ELISAs

416 using RBD from the Omicron variant and observed a reduction in anti-RBD IgG antibodies in
417 mRNA-vaccinated serum post-prime, and VLP-RBD-BECC serum at both time points (Fig.8C).
418 Omicron does not cause morbidity in the K18-hACE2 transgenic mouse model, negating
419 survival as a means of measuring protection in vaccine studies. To assess protection from VLP-
420 RBD-BECC compared to mRNA, mice were euthanized at 2 and 6 days after intranasal
421 challenge with 10^5 PFU Omicron to evaluate a reduction in viral replication. qRT-PCR analysis
422 of the viral nucleocapsid gene showed no difference between control and vaccinated groups in
423 the nasal wash or brain (data not shown). In the lung, viral RNA copy numbers were not
424 significantly different between Omicron-challenged control mice and IN VLP-RBD-BECC groups
425 at day 2 or day 6 (Fig.8D). However, viral replication, measured by plaque forming units in
426 mouse lung tissue, was significantly lower at day 2 in VLP-RBD-BECC mice than in the lung
427 tissue of controls (Fig.8E). By day 6, actively replicating virus was undetectable by plaque assay
428 in any group. These data together demonstrate that although our VLP-RBD-BECC vaccine
429 formulated using RBD from an ancestral virus elicits an antibody response that less-efficiently
430 targets the Omicron variant, the vaccine still reduces the development of viral burden in the lung
431 tissue of mice.

432 **Discussion**

433 As of the Fall of 2022, all COVID-19 vaccines approved for human use in the United States are
434 administered via the intramuscular route. Across the globe, however, countries such as China
435 and India have begun to approve a small number of intranasally-delivered platforms for use in
436 the continued fight against COVID-19, and even more are being actively evaluated in preclinical
437 and clinical trials [11]. Bharat Biotech's adenovirus vectored vaccine (formerly ChAd-SARS-
438 CoV-2-S, now BBV154) after extensive preclinical characterization was approved in India for
439 both primary vaccination and as a boost [38–40]. Another adenovirus vectored vaccine (Ad5-
440 nCoV-S) by CanSino Biologics in China was approved for use as an inhalable booster after

441 initial approval for intramuscular use, highlighting the potential to explore alternative routes of
442 administration with current vaccines to successfully incorporate intranasal vaccines into existing
443 vaccine schedules [41,42]. While administration of mRNA intranasally would be an attractive
444 approach to implementing an intranasal vaccine by repurposing an approved vaccine
445 formulation, the lipid nanoparticle shells of these vaccines are not formulated for
446 immunogenicity in the mucosa [12]. For intranasal use, vaccine platforms based on virus-like
447 particles which are highly immunogenic and incapable of replication (unlike adenoviruses or
448 lentiviruses making them safe for the elderly or immunocompromised), are a promising future
449 technology [43]. SpyBiotech developed a VLP-based vaccine for COVID-19 that, when
450 adjuvanted with alum or alum+CpG, conferred protection to rhesus macaque following SARS-
451 CoV-2 challenge [23,44]. The preclinical efficacy of this vaccine quickly prompted its
452 advancement to clinical trials, and here we have evaluated this antigen by intranasal route and
453 in combination with the BECC adjuvant.

454 In our study, we evaluated the combinatorial use of SpyBiotech's VLP-RBD, and the BECC 470
455 adjuvant, established by our lab to be an effective intranasal vaccine antigen in BReC-CoV-2,
456 as an intranasal vaccine for COVID-19. K18-hACE2 mice vaccinated with two doses of
457 intranasal VLP-RBD-BECC were protected against the development of severe disease and
458 morbidity after challenge with a lethal dose of the SARS-CoV-2 Delta variant. We demonstrated
459 that intranasal VLP-RBD-BECC elicits high anti-RBD IgG and IgA production, as compared to
460 intramuscular mRNA. The neutralizing activity of serum antibodies was lower in IN mice than
461 IM, but IN vaccination was still able to limit viral replication at 2 DPC. Viral RNA burden in the
462 lungs and nasal wash was reduced by IN vaccination at 10 DPC as compared to in NVC mice.
463 Importantly, IN vaccination prevented the dissemination of virus into the brain 10 DPC. Lung
464 inflammation, conferred potentially by the reduced production of the chemokine CXCL10, was
465 consistently limited after IN vaccination over the course of challenge studies (2 and 10 DPC).

466 Despite similarities in the viral RNA burden detectable in the lungs of IN and IM vaccinated mice
467 and similar scores for inflammation at day 10 post-challenge, IN VLP-RBD-BECC mice
468 displayed lower scores for lung inflammation at day 2 when compared to IM mRNA. Together
469 our data demonstrates that VLP-RBD-BECC administered via the intranasal route can provide
470 similar protection to mRNA-1273 against the Delta variant when administered intramuscularly.
471 While both intramuscular mRNA and intranasal VLP-RBD-BECC were able to fully protect mice
472 from challenge, future studies should evaluate the dose ranges and longevity of protection for
473 each vaccine formulation and vaccination scheme.

474 The hepatitis B surface antigen-based VLP-RBD used in this vaccine study utilized RBD from
475 an ancestral strain of SARS-CoV-2 (Wuhan/Washington-1). While currently approved COVID-19
476 vaccines on the market have utilized ancestral sequences and proteins of RBD and Spike, the
477 concept of matching vaccine antigen to challenge strain has recently gained more attention.
478 Emerging variants of SARS-CoV-2 acquire additional mutations to the viral Spike protein which
479 decreases the ability of neutralizing antibodies and other aspects of the immune system that
480 recognize the ancestral protein to recognize new variants like Omicron. Moderna and Pfizer-
481 BioNTech's bivalent mRNA booster vaccines were recently approved for use in the United
482 States as a means of enhancing variant-specific immunity [36,37]. Both vaccines conserve
483 inclusion of genetic material from the ancestral strain, but additionally contain genetic
484 sequences encoding the Omicron BA.4 and BA.5 variants. It's been largely reported that original
485 COVID-19 vaccines remained partially protective against severe disease against the Delta and
486 Omicron variants albeit with increased waning of protection over time [45]. We showed
487 previously that VLP-RBD with other adjuvants was protective intramuscularly against early
488 SARS-CoV-2 variants of concern [17]. Intranasal VLP-RBD-BECC was 100% protective against
489 lethal Delta challenge in the K18-hACE2 mouse, boasting the superiority of this vaccine as
490 compared to our BreC-CoV2 vaccine [16]. One area where intranasal VLP-RBD-BECC did not

491 outperform intramuscular mRNA was in *in vitro* RBD-ACE2 neutralization. Although neutralizing
492 antibodies from intranasal mice were high in serum post-boost and prevented Delta plaque
493 formation, and our *in vitro* binding assay showed high ACE2-RBD binding inhibition against
494 Delta when it was the challenge strain, vaccination-induced antibodies did not highly recognize
495 Omicron RBD and did not convey sterilizing immunity against early Omicron virus replication in
496 the lungs (at day 2). To meet our goal of developing a vaccination scheme that will improve
497 protection against highly transmissible viral variants, future studies with this platform would need
498 to assess the incorporation of VOC specific RBD into the VLP antigen before the vaccine moves
499 into other preclinical models like hamsters where we can assess additional correlates of
500 protection like reduced transmission.

501 Numerous intranasal vaccines utilizing a variety of platforms have been characterized in
502 preclinical K18-hACE2 mouse challenge experiments [14,16,54–58,46–53]. Intranasal vaccines
503 are also being developed by other labs to improve COVID-19 vaccines, although none reported
504 so far have utilized the virus-like particle, and none have been evaluated preclinically against
505 the highly virulent and pathogenic Delta variant. The adenovirus platform is another popular
506 option for intranasal vaccines due to its high immunogenicity. One dose of ChAd-SARS-CoV-2-
507 S, an adenovirus-based Spike protein-encoding vaccine that has progressed to evaluation in
508 human trials, was shown to be protective in mice, hamsters, and rhesus macaques [39,40,57].
509 Hassan, et al. reported that ChAd-SARS-CoV-2-S confers lasting immunity against SARS-CoV-
510 2 variants of concern using serological assays against variant strain RBD. Although dampened
511 compared to ancestral strains, ChAd-SARS-CoV-2-S induced neutralizing antibodies that bound
512 Delta [57]. To our knowledge, this vaccine and its correlates of protection have yet to be
513 evaluated authentically in a challenge study with the Delta variant. Vesin et al. evaluated the
514 protection of a lentiviral based Spike vaccine (Lv:S) as a boost in Ad5:hACE2 transfected mice
515 later challenged with the Delta variant [56]. Although this Delta challenge model did not utilize

516 the K18-hACE2 transgenic mouse that is susceptible to SARS-CoV-2 induced pathology, it did
517 show effective limitation of viral RNA post-challenge in the lung [56]. In these studies,
518 researchers assessed the added benefits of intranasal vaccination that exist in addition to
519 protection against morbidity and mortality. Immunogenicity studies for intranasal vaccines have
520 described that they are able to not only elicit high mucosal antibody levels, but important T cell
521 populations resident to the lung and respiratory tract [59]. This priming of the mucosa is likely a
522 major contributor to reducing early disease pathology—reduced viral replication in the upper
523 respiratory tract, limited lung inflammation, and decreased transmission/viral shedding—seen by
524 our lab and others. Vesin et al. evaluated the implementation of their IN Lv:S vaccine as a
525 booster in addition to a previously administered mRNA schedule [56]. This is an important
526 variable to consider as we work to implement intranasal vaccines into the long-term COVID-19
527 response as most of the world will be intramuscularly vaccinated and require additional
528 boosters. VLP-RBD-BECC could be an advantageous booster for COVID-19 protection due its
529 mucosal IgA responses which would supplement the strong IgG-dominant responses incurred
530 by mRNA priming. While VLP-RBD-BECC and mRNA were equally matched in their ability to
531 confer protection against SARS-CoV-2 challenge, we showed that antibody responses to both
532 vaccines were distinct. VLP-RBD-BECC as an intranasal vaccine primed the host for IgA
533 production, which was not seen in mRNA vaccinated mice, but mRNA vaccinated mice showed
534 higher IgG production systemically. IgA responses may provide better sterilizing immunity in the
535 mucosa, protecting against disease pathology and possibly even transmission in a manner
536 which systemic IgG levels cannot. The function of VLP-RBD-BECC induced IgA compared to
537 mRNA-induced IgG merits further study. Additionally, the BECC 470 adjuvant used in this
538 formulation was described to confer a Th1 dominant T cell response in BReC-CoV-2 which
539 could diversify the immune response to mRNA which is normally dominated by B cells [60].
540 Deeper cellular analyses using these vaccines could help shed light on their unique
541 mechanisms of protection. To further enhance the translational ability of this work, a model of

542 waning immunity would also need to be established to mimic the changes in memory responses
543 over time.

544 This VLP-RBD-BECC formulation shows promise as the COVID-19 pandemic progresses.
545 Additional immunogenicity studies using Omicron RBD or other emerging strain RBDs will be
546 necessary to improve the neutralizing antibody responses suggested by this challenge study. In
547 these future immunogenicity studies, it will also be important to characterize the tissue-specific
548 T cell responses to vaccination. Lung-resident T regulatory and T memory cells are vital to the
549 lasting protection against SARS-CoV-2 [61–63]. Investigation of the neutralizing abilities of
550 vaccine-induced IgA responses will also be interesting for describing not just the mechanistic
551 ability of VLP-RBD-BECC to induce protection, but for also characterizing the potential of
552 intranasal vaccines against other pathogens.

553 **Figure Legends**

554 **Figure 1: Intranasal VLP-RBD-BECC induces strong antibody responses in K18-hACE2**
555 **mice.** Anti-RBD IgG levels were measured in serum A) four weeks post-prime vaccination, and
556 B) four weeks post-boost vaccination (n=10 mice per group). Serum, nasal wash, and lung
557 supernatant were collected at euthanasia points (NVC mice reached total morbidity by day 6
558 while all other groups survived to day 10 post-challenge) to measure C) serum anti-RBD IgG, D)
559 serum anti-RBD IgA, E) nasal wash anti-RBD IgA, and F) lung supernatant anti-RBD IgA (n=7
560 mice euthanized at 6 or 10 DPC). Each point denotes one biological replicate. One Way
561 ANOVA with Tukey's Multiple Comparisons was performed to determine *P* value: *****P*<0.0001,
562 ****P*<0.0006, ***P*=0.0063

563 **Figure 2: Neutralizing antibodies against multiple SARS-CoV-2 VOC RBD are elicited**
564 **from IN VLP-RBD-BECC.** A) Serum IgG antibodies from mRNA or VLP-RBD-BECC vaccinated
565 mice were analyzed at euthanasia point 6 (NVC) or 10 (IM mRNA or IN VLP-RBD-BECC) days

566 post-challenge to measure *in vitro* ACE2-RBD % binding inhibition and compared to PBS-
567 vaccinated and challenged mice. Points represent the average of n=6-7 biological replicates.
568 Unpaired T tests were performed for statistical analysis: * = significance between mRNA and
569 VLP-RBD-BECC at dilution point ($P<0.05$). B) The PRNT50 (percent neutralization 50) values
570 were interpolated for each biological replicate from the dilution curve of % binding inhibition. way
571 ANOVA with Tukey's Multiple Comparisons was performed for statistical analysis. *** $P<0.0091$,
572 ** $P=0.0020$.

573 **Figure 3: Serum from VLP-RBD-BECC vaccinated mice reduce plaque formation *in vitro*.**

574 Serum collected 4 weeks post-boost was added with Delta SARS-CoV-2 (n=10 biological
575 samples per group) to Vero E6-AT cells to measure the ability of antibodies to reduce plaque
576 formation. Unpaired t-tests were performed for statistical analysis: * $P<0.05$

577 **Figure 4: Vaccination with VLP-RBD-BECC intranasally confers protection against lethal**

578 **challenge with Delta.** A) Mice were monitored daily for disease progression after challenge
579 with the sum of their disease scores reported daily for up to 10 days post-challenge. B) Daily
580 weight and C) temperature change was measured to monitor disease. Mice in the NVC group
581 reached morbidity by day 6 at which point disease scores stopped being reported. Any mice
582 euthanized before complete euthanasia of the group had their score retained for reporting. D)
583 Kaplan Meier survival curve of vaccinated and viral-challenged K18-hACE2 mice. (n=7 mice per
584 group)

585 **Figure 5: IN VLP-RBD-BECC and IM mRNA limit viral replication and tissue viral burden.**

586 A) PFUs from lung homogenates of mice euthanized 2 days post-challenge (n=3 mice per
587 group). B) qRT-PCR was performed to measure viral RNAs in the nasal wash, C) lung and D)
588 brain of mice in each experimental group euthanized at day 2 post-challenge or at euthanasia.
589 Mice in the NVC group all reached morbidity by day 6 (symbols outlined in red) while all other
590 groups survived to day 10. Copy numbers calculated below the limit of detection (LOD

591 designated by dashed line) were set as equal to the LOD for reporting. One way ANOVA with
592 Tukey's Multiple Comparisons was performed for statistical analysis. **** $P<0.0001$,
593 *** $P=0.0003$, ** $P=0.0066$, * $P=0.0445$. (n=3 mice per group euthanized at 2 DPC, n=7 mice
594 euthanized humane endpoint or 10 DPC)

595 **Figure 6: Vaccination limits CXCL10 production in the lung after Delta variant challenge.**

596 CXCL10 concentrations were quantified in the A) serum and B) lung supernatant of K18-hACE2
597 mice 2 or 10 days after SARS-CoV-2 viral challenge (NVC mice surviving past 2 DPC were
598 euthanized 4-6 DPC). Each symbol represents one biological replicate. One way ANOVA with
599 Tukey's Multiple Comparisons was performed for statistical analysis. **** $P<0.0001$, *** $P<0.0003$
600 ** $P<0.0013$

601 **Figure 7: Histopathological analysis shows lung inflammation is limited by VLP-RBD-**

602 **BECC in SARS-CoV-2 challenged mice.** A) Representative images of H&E-stained mouse
603 lungs collected at euthanasia after viral challenge. Total inflammation scores comprised of acute
604 and chronic inflammation scores were awarded to mice euthanized B) two (n=3) or C) 10 days
605 (n=7) post-challenge (NVC mice surviving past 2 DPC were euthanized on or before 6 DPC).
606 For each parameter of acute and chronic inflammation, 0=none; 1=minimal; 2=mild;
607 3=moderate; 4=marked; 5=severe. D) Margination of immune cells into the blood vessels was
608 scored for each mouse where 0=none; 1=mild; 2=moderate; 3=severe. Statistical analyses were
609 performed using one way ANOVA with Tukey's Multiple Comparisons: **** $P<0.0001$, * $P<0.0295$

610 **Figure 8: Protection from VLP-RBD-BECC is reduced against Omicron challenge.** A) *In*

611 *vitro* binding inhibition assays were performed to measure the binding of serum IgG antibodies
612 collected two weeks post boost to Omicron RBD. Points denote the average of n=6 biological
613 replicates, Unpaired T tests were performed for statistical analysis: * = significance between
614 mRNA and VLP-RBD-BECC at dilution point ($P<0.05$). B) Anti-Wuhan RBD IgG antibodies and
615 C) anti-Omicron RBD IgG antibodies were quantified by ELISA in serum two weeks post prime

616 and two weeks post boost. D) qRT-PCR analysis was performed to determine copy number of
617 the SARS-CoV-2 nucleocapsid gene in lung tissue homogenates collected 2- or 6-days post-
618 challenge. Dashed lines indicate the limit of detection. E) Plaque assays were performed using
619 lung tissue supernatant collected 2- or 6-days post-challenge to measure viral burden. Each
620 point denotes one biological replicate. One Way ANOVA with Tukey's Multiple Comparisons
621 was performed to determine P value: **** $P < 0.0001$, *** $P < 0.0006$, ** $P = 0.0017$

622 **Acknowledgments**

623 We thank Drs. Laura Gibson and Clay Marsh of the West Virginia University Health Sciences
624 Center for their support of COVID-19 preclinical research efforts. We would like to thank Drs.
625 Matthew D.J. Dicks and Sumi Biswas (SpyBiotech) for the use of their VLP-RBD platform and
626 Dr. Robert Ernst for the use of the BECC adjuvant. We thank Dr. Christopher Love (MIT) for
627 providing the Spytagged RBD used in the VLP-RBD. We thank Dr. Ivan Martinez and Michael
628 Winters for propagating the original challenge strain of the SARS-CoV-2 Delta variant, and Dr.
629 Luis Martinez-Sobrido and Dr. Jordi Torrelles from the Texas Biomedical Research Institute for
630 providing us with stocks of the Omicron variant for preclinical challenge studies. We would also
631 like to acknowledge Mary Tomago-Chesney for her preparation of lung tissues for histology. We
632 want to thank WVU's Electron Microscopy, Histopathology and Tissue Bank Core for the images
633 of lung tissues. The preparation of figures for this manuscript was supported by GraphPad
634 Prism and BioRender.

635 **Funding**

636 F.H.D. and the Vaccine Development Center (VDC) are supported by Research Challenge grant
637 number HEPC.dsr.18.6 from the Division of Science and Research, West Virginia Higher
638 Education Policy Commission. MSD QuickPlex SQ120 in the West Virginia University (WVU)
639 Flow Cytometry & Single Cell Core Facility is supported by the Institutional Development

640 Awards (IDeA) from the National Institute of General Medical Sciences of the National Institutes
641 of Health under grant numbers P30GM121322 (TME CoBRE) and P20GM103434 751 (INBRE).

642 **Author Contributions**

643 These studies were designed by FHD, KSL, TYW and JRB. The BECC470 adjuvant was
644 developed and provided by RKE. Viral strains were propagated and sequenced by MTW and
645 IM. Mouse challenge studies as well as the subsequent necropsy and tissue processing were
646 performed by KSL, OAM and MC. ELISAs were performed by NAR, OAM, and KSL. MC
647 performed plaque assays, plaque reduction assays, and *in vitro* antibody neutralization assays.
648 qRT-PCR of tissue viral RNA was performed by OAM. Luminex assays were performed by KSL.
649 Histopathological analyses of lung tissues were carried out by MSA. The data in this manuscript
650 was prepared by KSL and FHD. All authors contributed to the writing and revision of this
651 manuscript.

652 **References**

- 653 [1] Zuckerman JN. The importance of injecting vaccines into muscle□: Different patients
654 need different needle sizes. *BMJ Br Med J* 2000;321:1237.
655 <https://doi.org/10.1136/BMJ.321.7271.1237>.
- 656 [2] Pollard AJ, Bijker EM. A guide to vaccinology: from basic principles to new developments.
657 *Nat Rev Immunol* 2020 212 2020;21:83–100. [https://doi.org/10.1038/s41577-020-00479-](https://doi.org/10.1038/s41577-020-00479-7)
658 [7](https://doi.org/10.1038/s41577-020-00479-7).
- 659 [3] Rosenbaum P, Tchitchek N, Joly C, Rodriguez Pozo A, Stimmer L, Langlois S, et al.
660 Vaccine Inoculation Route Modulates Early Immunity and Consequently Antigen-Specific
661 Immune Response. *Front Immunol* 2021;12:1362.
662 <https://doi.org/10.3389/FIMMU.2021.645210/BIBTEX>.

- 663 [4] Ols S, Yang L, Thompson EA, Pushparaj P, Tran K, Liang F, et al. Route of Vaccine
664 Administration Alters Antigen Trafficking but Not Innate or Adaptive Immunity. *Cell Rep*
665 2020;30:3964-3971.e7. <https://doi.org/10.1016/J.CELREP.2020.02.111>.
- 666 [5] Alu A, Chen L, Yuquan HL, Tian WX, Wei X. Intranasal COVID-19 vaccines: From bench
667 to bed-NC-ND license (<http://creativecommons.org/licenses/by-nc-nd/4.0/>) 2022.
668 <https://doi.org/10.1016/j>.
- 669 [6] Redfield RR, Kenzie WR Mac, Kent CK, Leahy MA, Martinroe JC, Spriggs SR, et al.
670 Prevention and Control of Seasonal Influenza with Vaccines: Recommendations of the
671 Advisory Committee on Immunization Practices-United States, 2018-19 Influenza Season
672 Morbidity and Mortality Weekly Report Recommendations and Reports Centers for
673 Disease Control and Prevention MMWR Editorial and Production Staff (Serials) MMWR
674 Editorial Board CDC Adoption of ACIP Recommendations for MMWR Recommendations
675 and Reports, MMWR Policy Notes, and Immunization Schedules (Child/Adolescent,
676 Adult) 2018.
- 677 [7] Lavelle EC, Ward RW. Mucosal vaccines — fortifying the frontiers. *Nat Rev Immunol*
678 2021 224 2021;22:236–50. <https://doi.org/10.1038/s41577-021-00583-2>.
- 679 [8] Waltz E. How nasal-spray vaccines could change the pandemic. *Nature* 2022;609:240–2.
680 <https://doi.org/10.1038/D41586-022-02824-3>.
- 681 [9] Topol EJ, Iwasaki A. Operation Nasal Vaccine—Lightning speed to counter COVID-19.
682 *Sci Immunol* 2022;7. [https://doi.org/10.1126/SCIIMMUNOL.ADD9947/ASSET/99E73652-
683 A709-495C-92AA-1B8A0B05A7E5/ASSETS/IMAGES/LARGE/SCIIMMUNOL.ADD9947-
684 FB.JPG](https://doi.org/10.1126/SCIIMMUNOL.ADD9947/ASSET/99E73652-A709-495C-92AA-1B8A0B05A7E5/ASSETS/IMAGES/LARGE/SCIIMMUNOL.ADD9947-FB.JPG).
- 685 [10] Evans JP, Zeng C, Carlin C, Lozanski G, Saif LJ, Oltz EM, et al. Neutralizing antibody
686 responses elicited by SARS-CoV-2 mRNA vaccination wane over time and are boosted

- 687 by breakthrough infection. *Sci Transl Med* 2022;14:8057.
- 688 https://doi.org/10.1126/SCITRANSLMED.ABN8057/SUPPL_FILE/SCITRANSLMED.ABN
- 689 [8057_MDAR_REPRODUCIBILITY_CHECKLIST.ZIP](https://doi.org/10.1126/SCITRANSLMED.ABN8057/SUPPL_FILE/SCITRANSLMED.ABN8057_MDAR_REPRODUCIBILITY_CHECKLIST.ZIP).
- 690 [11] Waltz E. China and India approve nasal COVID vaccines — are they a game changer?
- 691 *Nature* 2022. <https://doi.org/10.1038/D41586-022-02851-0>.
- 692 [12] Mao T, Israelow B, Peña-Hernández MA, Suberi A, Zhou L, Luyten S, et al.
- 693 Unadjuvanted intranasal spike vaccine elicits protective mucosal immunity against
- 694 sarbecoviruses. *Science* (80-) 2022. <https://doi.org/10.1126/SCIENCE.ABO2523>.
- 695 [13] Christensen D, Polacek C, Sheward DJ, Hanke L, Moliner-Morro A, McInerney G, et al.
- 696 Protection against SARS-CoV-2 transmission by a parenteral prime—Intranasal boost
- 697 vaccine strategy. *EBioMedicine* 2022;84:104248.
- 698 <https://doi.org/10.1016/j.ebiom.2022.104248>.
- 699 [14] Zhou R, Wang P, Wong YC, Xu H, Lau SY, Liu L, et al. Nasal prevention of SARS-CoV-2
- 700 infection by intranasal influenza-based boost vaccination in mouse models. *EBioMedicine*
- 701 2022;75:103762. <https://doi.org/10.1016/j.ebiom.2021.103762>.
- 702 [15] Zhao J, Zhao J, Mangalam AK, Channappanavar R, Fett C, Meyerholz DK, et al. Airway
- 703 Memory CD4+ T Cells Mediate Protective Immunity against Emerging Respiratory
- 704 Coronaviruses. *Immunity* 2016;44:1379–91.
- 705 <https://doi.org/10.1016/J.IMMUNI.2016.05.006>.
- 706 [16] Wong TY, Lee KS, Russ BP, Horspool AM, Kang J, Winters MT, et al. Intranasal
- 707 administration of BReC-CoV-2 COVID-19 vaccine protects K18-hACE2 mice against
- 708 lethal SARS-CoV-2 challenge. *NPJ Vaccines* 2022;7. [https://doi.org/10.1038/S41541-](https://doi.org/10.1038/S41541-022-00451-7)
- 709 [022-00451-7](https://doi.org/10.1038/S41541-022-00451-7).

- 710 [17] Wong TY, Russ BP, Lee KS, Miller OA, Kang J, Cooper M, et al. RBD-VLP Vaccines
711 Adjuvanted with Alum or SWE Protect K18-hACE2 Mice against SARS-CoV-2 VOC
712 Challenge. *MSphere* 2022;7. <https://doi.org/10.1128/MSPHERE.00243-22>.
- 713 [18] Gregg KA, Harberts E, Gardner FM, Pelletier MR, Cayatte C, Yu L, et al. Rationally
714 designed TLR4 ligands for vaccine adjuvant discovery. *MBio* 2017;8.
715 <https://doi.org/10.1128/mBio.00492-17>.
- 716 [19] Gregg KA, Harberts E, Gardner FM, Pelletier MR, Cayatte C, Yu L, et al. A lipid A-based
717 TLR4 mimetic effectively adjuvants a *Yersinia pestis* rF-V1 subunit vaccine in a murine
718 challenge model. *Vaccine* 2018;36:4023.
719 <https://doi.org/10.1016/J.VACCINE.2018.05.101>.
- 720 [20] Hotez PJ, Bottazzi ME. Developing a low-cost and accessible COVID-19 vaccine for
721 global health. *PLoS Negl Trop Dis* 2020;14:e0008548.
722 <https://doi.org/10.1371/JOURNAL.PNTD.0008548>.
- 723 [21] Love KR, Dalvie NC, Love JC. The yeast stands alone: the future of protein biologic
724 production. *Curr Opin Biotechnol* 2018;53:50–8.
725 <https://doi.org/10.1016/j.copbio.2017.12.010>.
- 726 [22] Dalvie NC, Biedermann AM, Rodriguez-Aponte SA, Naranjo CA, Rao HD, Rajurkar MP,
727 et al. Scalable, methanol-free manufacturing of the SARS-CoV-2 receptor-binding domain
728 in engineered *Komagataella phaffii*. *Biotechnol Bioeng* 2022;119:657–62.
729 <https://doi.org/10.1002/BIT.27979>.
- 730 [23] Dalvie NC, Tostanoski LH, Rodriguez-Aponte SA, Kaur K, Bajoria S, Kumru OS, et al.
731 SARS-CoV-2 receptor binding domain displayed on HBsAg virus-like particles elicits
732 protective immunity in macaques. *Sci Adv* 2022;8:6015.
733 <https://doi.org/10.1126/SCIADV.ABL6015>.

- 734 [24] Singh SK, Thrane S, Janitzek CM, Nielsen MA, Theander TG, Theisen M, et al.
735 Improving the malaria transmission-blocking activity of a Plasmodium falciparum 48/45
736 based vaccine antigen by SpyTag/SpyCatcher mediated virus-like display. *Vaccine*
737 2017;35:3726–32. <https://doi.org/10.1016/J.VACCINE.2017.05.054>.
- 738 [25] Wong TYT, Lee KSK, Russ B, Horspool AMA, Kang JK, Winters M, et al. Intranasal
739 administration of BReC-CoV-2 COVID-19 vaccine protects K18-hACE2 mice against
740 lethal SARS-CoV-2 challenge [Accepted Jan. 20, 2022 PMID: PMC Journal - In
741 Process]. *Npj Vaccines* 2022.
- 742 [26] Case JB, Bailey AL, Kim AS, Chen RE, Diamond MS. Growth, detection, quantification,
743 and inactivation of SARS-CoV-2. *Virology* 2020;548:39–48.
744 <https://doi.org/10.1016/j.virol.2020.05.015>.
- 745 [27] Lee KS, Wong TY, Russ BP, Horspool AM, Miller OA, Rader NA, et al. SARS-CoV-2
746 Delta variant induces enhanced pathology and inflammatory responses in K18-hACE2
747 mice. *PLoS One* 2022;17:e0273430. <https://doi.org/10.1371/JOURNAL.PONE.0273430>.
- 748 [28] Lee KS, Russ BP, Wong TY, Horspool AM, Winters MT, Barbier M, et al. Obesity and
749 metabolic dysfunction drive sex-associated differential disease profiles in hACE2-mice
750 challenged with SARS-CoV-2. *IScience* 2022;25:105038.
751 <https://doi.org/10.1016/J.ISCI.2022.105038>.
- 752 [29] Corbett KS, Nason MC, Flach B, Gagne M, O'Connell S, Johnston TS, et al. Immune
753 correlates of protection by mRNA-1273 vaccine against SARS-CoV-2 in nonhuman
754 primates. *Science (80-)* 2021;373.
755 https://doi.org/10.1126/SCIENCE.ABJ0299/SUPPL_FILE/SCIENCE.ABJ0299_Mدار_R
756 [EPRODUCIBILITY_CHECKLIST.PDF](https://doi.org/10.1126/SCIENCE.ABJ0299/SUPPL_FILE/SCIENCE.ABJ0299_Mدار_R).
- 757 [30] Wisnewski A V., Luna JC, Redlich CA. Human IgG and IgA responses to COVID-19

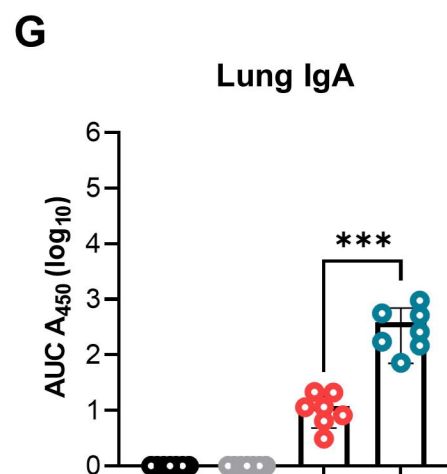
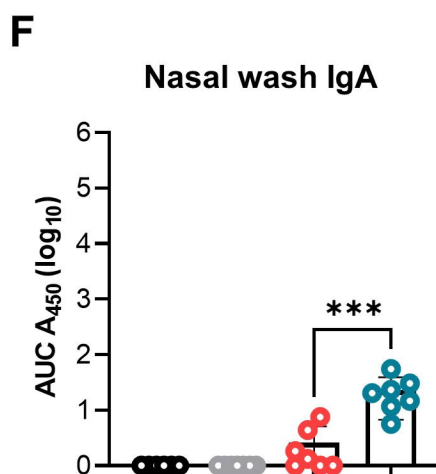
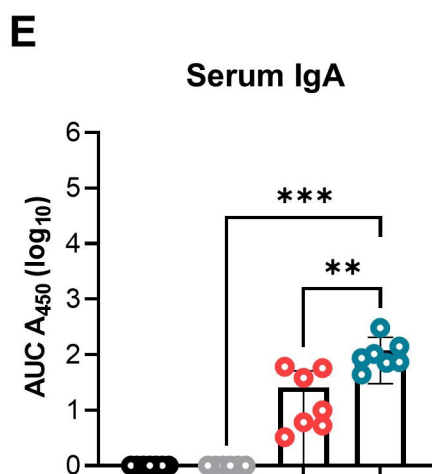
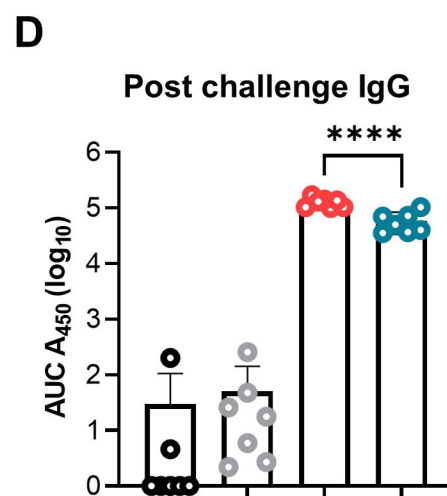
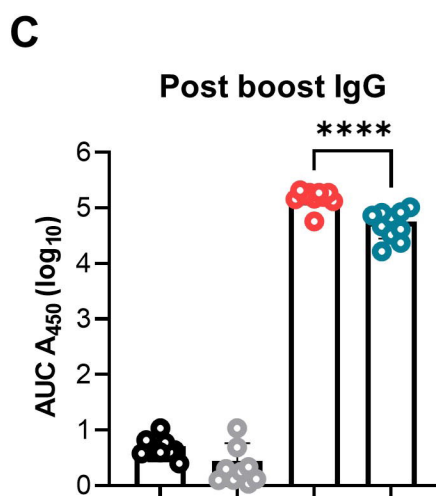
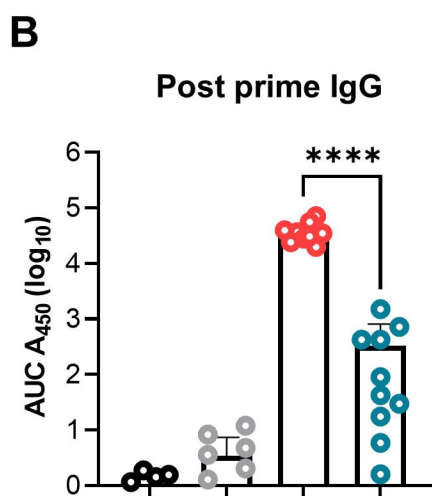
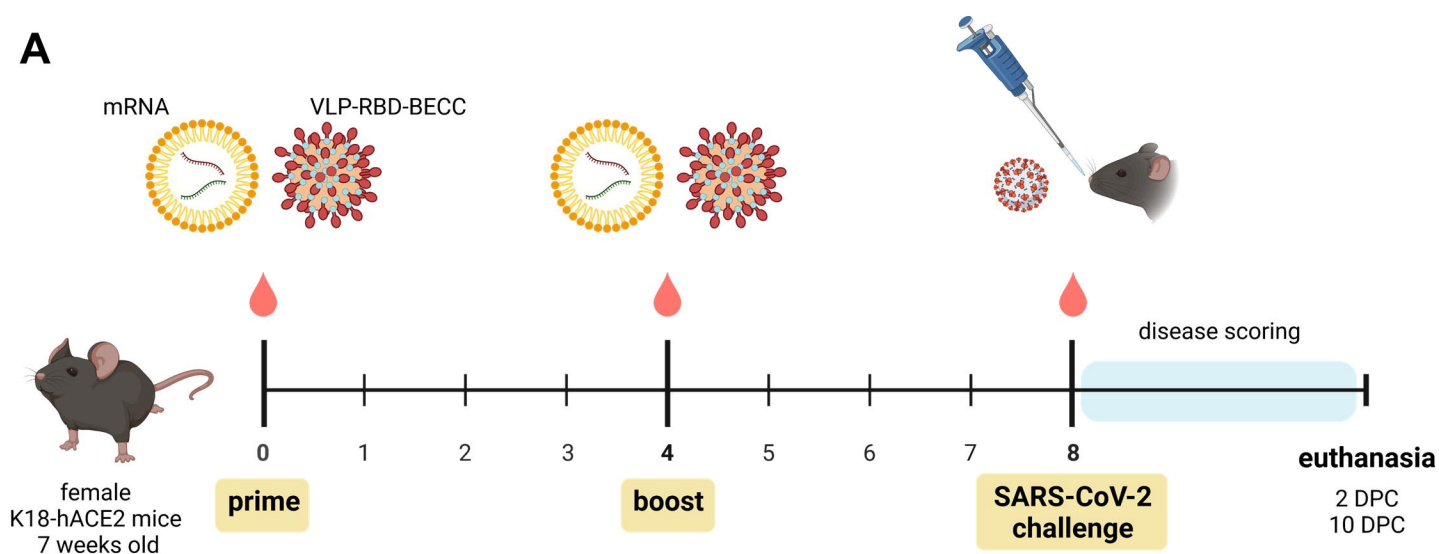
- 758 mRNA vaccines. *PLoS One* 2021;16:e0249499.
759 <https://doi.org/10.1371/JOURNAL.PONE.0249499>.
- 760 [31] Wong TY, Horspool AM, Russ BP, Ye C, Lee KS, Winters MT, et al. Evaluating antibody
761 mediated protection against Alpha, Beta, and Delta SARS-CoV-2 variants of concern in
762 K18-hACE2 transgenic mice 2022;96:2184–205. <https://doi.org/10.1128/JVI.02184-21>.
- 763 [32] Diamond M, Halfmann P, Maemura T, Iwatsuki-Horimoto K, Iida S, Kiso M, et al. The
764 SARS-CoV-2 B.1.1.529 Omicron virus causes attenuated infection and disease in mice
765 and hamsters. *Res Sq* 2021. <https://doi.org/10.21203/rs.3.rs-1211792/v1>.
- 766 [33] Liu X, Mostafavi H, Ng WH, Freitas JR, King NJC, Zaid A, et al. The Delta SARS-CoV-2
767 Variant of Concern Induces Distinct Pathogenic Patterns of Respiratory Disease in K18-
768 hACE2 Transgenic Mice Compared to the Ancestral Strain from Wuhan. *MBio* 2022.
769 <https://doi.org/10.1128/MBIO.00683-22>.
- 770 [34] Gudowska-Sawczuk M, Mroczko B. What Is Currently Known about the Role of CXCL10
771 in SARS-CoV-2 Infection? *Int J Mol Sci* 2022;23. <https://doi.org/10.3390/IJMS23073673>.
- 772 [35] Lorè NI, De Lorenzo R, Rancoita PMV, Cugnata F, Agresti A, Benedetti F, et al. CXCL10
773 levels at hospital admission predict COVID-19 outcome: hierarchical assessment of 53
774 putative inflammatory biomarkers in an observational study. *Mol Med* 2021;27:1–10.
775 <https://doi.org/10.1186/S10020-021-00390-4/FIGURES/6>.
- 776 [36] Scheaffer SM, Lee D, Whitener B, Ying B, Wu K, Liang C-Y, et al. Bivalent SARS-CoV-2
777 mRNA vaccines increase breadth of neutralization and protect against the BA.5 Omicron
778 variant in mice. *Nat Med* 2022 2022:1–1. <https://doi.org/10.1038/s41591-022-02092-8>.
- 779 [37] Chalkias S, Harper C, Vrbicky K, Walsh SR, Essink B, Brosz A, et al. A Bivalent Omicron-
780 Containing Booster Vaccine against Covid-19. *N Engl J Med* 2022;387.

- 781 <https://doi.org/10.1056/NEJMOA2208343>.
- 782 [38] Hassan AO, Feldmann F, Zhao H, Curiel DT, Okumura A, Tang-Huau TL, et al. A single
783 intranasal dose of chimpanzee adenovirus-vectored vaccine protects against SARS-CoV-
784 2 infection in rhesus macaques. *Cell Reports Med* 2021;2:100230.
785 <https://doi.org/10.1016/J.XCRM.2021.100230>.
- 786 [39] Hassan AO, Kafai NM, Dmitriev IP, Fox JM, Smith BK, Harvey IB, et al. A Single-Dose
787 Intranasal ChAd Vaccine Protects Upper and Lower Respiratory Tracts against SARS-
788 CoV-2. *Cell* 2020;183:169-184.e13. <https://doi.org/10.1016/J.CELL.2020.08.026>.
- 789 [40] Bricker TL, Darling TL, Hassan AO, Harastani HH, Soung A, Jiang X, et al. A single
790 intranasal or intramuscular immunization with chimpanzee adenovirus-vectored SARS-
791 CoV-2 vaccine protects against pneumonia in hamsters. *Cell Rep* 2021;36.
792 <https://doi.org/10.1016/J.CELREP.2021.109400>.
- 793 [41] Inhalable vaccine in trials n.d. <https://www.nature.com/articles/d42473-022-00043-y>
794 (accessed November 3, 2022).
- 795 [42] Li J, Hou L, Guo X, Jin P, Wu S, Zhu J, et al. Heterologous AD5-nCOV plus CoronaVac
796 versus homologous CoronaVac vaccination: a randomized phase 4 trial. *Nat Med* 2022
797 282 2022;28:401–9. <https://doi.org/10.1038/s41591-021-01677-z>.
- 798 [43] Nooraei S, Bahrulolum H, Hoseini ZS, Katalani C, Hajizade A, Easton AJ, et al. Virus-like
799 particles: preparation, immunogenicity and their roles as nanovaccines and drug
800 nanocarriers. *J Nanobiotechnology* 2021 191 2021;19:1–27.
801 <https://doi.org/10.1186/S12951-021-00806-7>.
- 802 [44] Tan TK, Rijal P, Rahikainen R, Keeble AH, Schimanski L, Hussain S, et al. A COVID-19
803 vaccine candidate using SpyCatcher multimerization of the SARS-CoV-2 spike protein

- 804 receptor-binding domain induces potent neutralising antibody responses. *Nat Commun*
805 2021;12:1–16. <https://doi.org/10.1038/s41467-020-20654-7>.
- 806 [45] Andrews N, Stowe J, Kirsebom F, Toffa S, Rickeard T, Gallagher E, et al. Covid-19
807 Vaccine Effectiveness against the Omicron (B.1.1.529) Variant. *N Engl J Med*
808 2022;386:1532–46.
809 https://doi.org/10.1056/NEJMOA2119451/SUPPL_FILE/NEJMOA2119451_DISCLOSUR
810 ES.PDF.
- 811 [46] Ewer KJ, Barrett JR, Belij-Rammerstorfer S, Sharpe H, Makinson R, Morter R, et al. T cell
812 and antibody responses induced by a single dose of ChAdOx1 nCoV-19 (AZD1222)
813 vaccine in a phase 1/2 clinical trial. *Nat Med* 2021;27:270–8.
814 <https://doi.org/10.1038/S41591-020-01194-5>.
- 815 [47] Tukhvatulin AI, Gordeychuk I V., Dolzhikova I V., Dzharullaeva AS, Krasina ME,
816 Bayurova EO, et al. Immunogenicity and protectivity of intranasally delivered vector-
817 based heterologous prime-boost COVID-19 vaccine Sputnik V in mice and non-human
818 primates. *Emerg Microbes Infect* 2022;11:2229–47.
819 <https://doi.org/10.1080/22221751.2022.2119169>.
- 820 [48] Seo SH, Jang Y. Cold-Adapted Live Attenuated SARS-Cov-2 Vaccine Completely
821 Protects Human ACE2 Transgenic Mice from SARS-Cov-2 Infection. *Vaccines* 2020;8:1–
822 17. <https://doi.org/10.3390/VACCINES8040584>.
- 823 [49] Schultz MD, Suschak JJ, Botta D, Silva-Sanchez A, King RG, Detchemendy TW, et al. A
824 single intranasal administration of AdCOVID protects against SARS-CoV-2 infection in
825 the upper and lower respiratory tracts. *Hum Vaccin Immunother* 2022.
826 <https://doi.org/10.1080/21645515.2022.2127292>.
- 827 [50] King RG, Silva-Sanchez A, Peel JN, Botta D, Dickson AM, Pinto AK, et al. Single-Dose

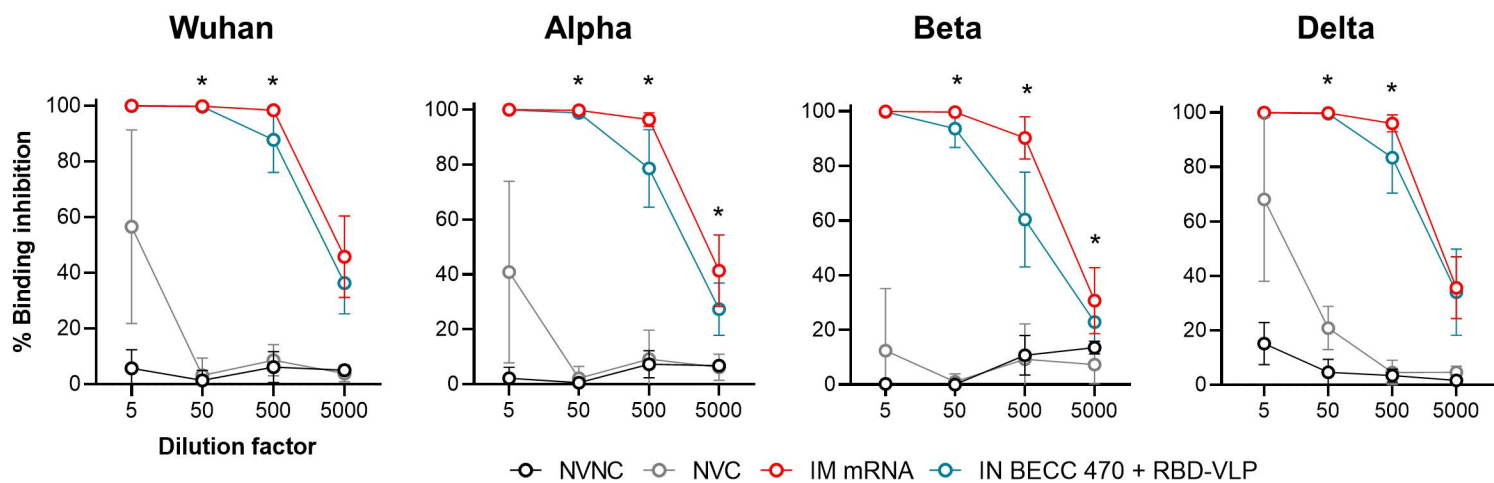
- 828 Intranasal Administration of AdCOVID Elicits Systemic and Mucosal Immunity against
829 SARS-CoV-2 and Fully Protects Mice from Lethal Challenge. *Vaccines* 2021;9.
830 <https://doi.org/10.3390/VACCINES9080881>.
- 831 [51] Pérez P, Astorgano D, Albericio G, Flores S, Sánchez-Cordón PJ, Luczkowiak J, et al.
832 Intranasal administration of a single dose of MVA-based vaccine candidates against
833 COVID-19 induced local and systemic immune responses and protects mice from a lethal
834 SARS-CoV-2 infection. *Front Immunol* 2022;13.
835 <https://doi.org/10.3389/FIMMU.2022.995235>.
- 836 [52] Americo JL, Cotter CA, Earl PL, Liu R, Moss B. Intranasal inoculation of an MVA-based
837 vaccine induces IgA and protects the respiratory tract of hACE2 mice from SARS-CoV-2
838 infection. *Proc Natl Acad Sci U S A* 2022;119. <https://doi.org/10.1073/PNAS.2202069119>.
- 839 [53] An D, Li K, Rowe DK, Diaz MCH, Griffin EF, Beavis AC, et al. Protection of K18-hACE2
840 mice and ferrets against SARS-CoV-2 challenge by a single-dose mucosal immunization
841 with a parainfluenza virus 5-based COVID-19 vaccine. *Sci Adv* 2021;7.
842 <https://doi.org/10.1126/SCIADV.ABI5246>.
- 843 [54] Cao H, Mai J, Zhou Z, Li Z, Duan R, Watt J, et al. Intranasal HD-Ad vaccine protects the
844 upper and lower respiratory tracts of hACE2 mice against SARS-CoV-2. *Cell Biosci*
845 2021;11. <https://doi.org/10.1186/S13578-021-00723-0>.
- 846 [55] Jiang L, Driedonks TAP, Jong WSP, Dhakal S, Bart van den Berg van Saparoea H,
847 Sitaras I, et al. A bacterial extracellular vesicle-based intranasal vaccine against SARS-
848 CoV-2 protects against disease and elicits neutralizing antibodies to wild-type and Delta
849 variants. *J Extracell Vesicles* 2022;11:e12192. <https://doi.org/10.1002/JEV2.12192>.
- 850 [56] Vesin B, Lopez J, Noirat A, Authié P, Fert I, Le Chevalier F, et al. An intranasal lentiviral
851 booster reinforces the waning mRNA vaccine-induced SARS-CoV-2 immunity that it

- 852 targets to lung mucosa 2022. <https://doi.org/10.1016/j.ymthe.2022.04.016>.
- 853 [57] Hassan AO, Shrihari S, Gorman MJ, Ying B, Yaun D, Raju S, et al. An intranasal vaccine
854 durably protects against SARS-CoV-2 variants in mice. *Cell Rep* 2021;36:109452.
855 <https://doi.org/10.1016/J.CELREP.2021.109452>.
- 856 [58] An X, Martinez-Paniagua M, Rezvan A, Sefat SR, Fathi M, Singh S, et al. Single-dose
857 intranasal vaccination elicits systemic and mucosal immunity against SARS-CoV-2.
858 *IScience* 2021;24:103037. <https://doi.org/10.1016/J.ISCI.2021.103037>.
- 859 [59] Lapuente D, Fuchs J, Willar J, Vieira Antão A, Eberlein V, Uhlig N, et al. Protective
860 mucosal immunity against SARS-CoV-2 after heterologous systemic prime-mucosal
861 boost immunization. *Nat Commun* 2021 121 2021;12:1–14.
862 <https://doi.org/10.1038/s41467-021-27063-4>.
- 863 [60] Heinz FX, Stiasny K. Distinguishing features of current COVID-19 vaccines: knowns and
864 unknowns of antigen presentation and modes of action. *Npj Vaccines* 2021 61 2021;6:1–
865 13. <https://doi.org/10.1038/s41541-021-00369-6>.
- 866 [61] Sette A, Crotty S. Adaptive immunity to SARS-CoV-2 and COVID-19. *Cell* 2021;184:861–
867 80. <https://doi.org/10.1016/J.CELL.2021.01.007>.
- 868 [62] Bertoletti A, Le Bert N, Tan AT. SARS-CoV-2-specific T cells in the changing landscape
869 of the COVID-19 pandemic. *Immunity* 2022;55.
870 <https://doi.org/10.1016/J.IMMUNI.2022.08.008>.
- 871 [63] Neidleman J, Luo X, McGregor M, Xie G, Murray V, Greene WC, et al. mRNA vaccine-
872 induced T cells respond identically to SARS-CoV-2 variants of concern but differ in
873 longevity and homing properties depending on prior infection status. *Elife* 2021;10.
874 <https://doi.org/10.7554/ELIFE.72619>.

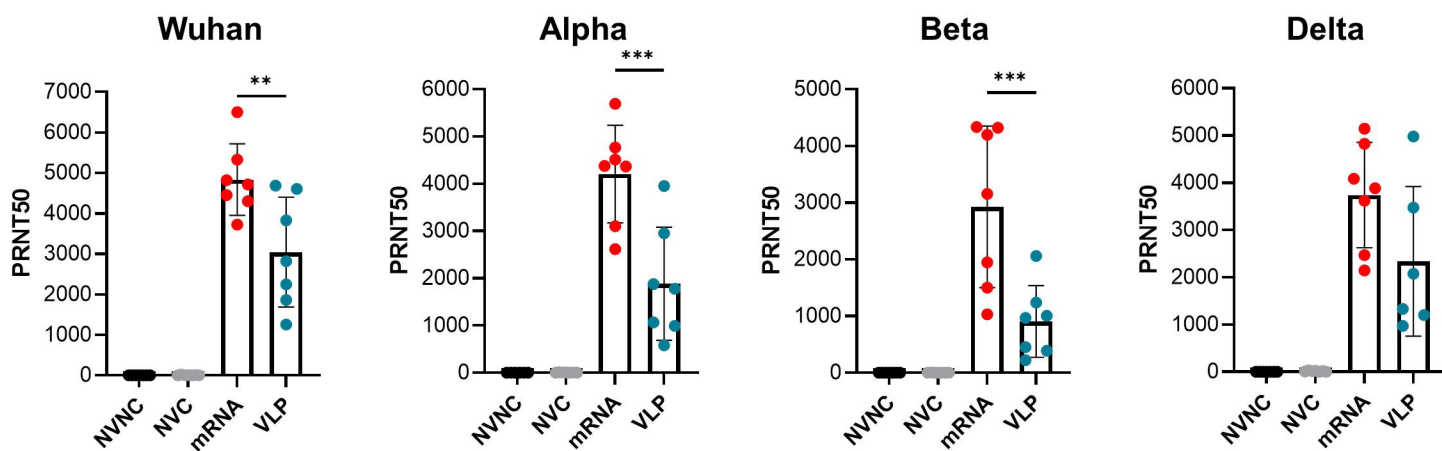


● NVNC ● NVC ● IM mRNA ● IN VLP-RBD-BECC

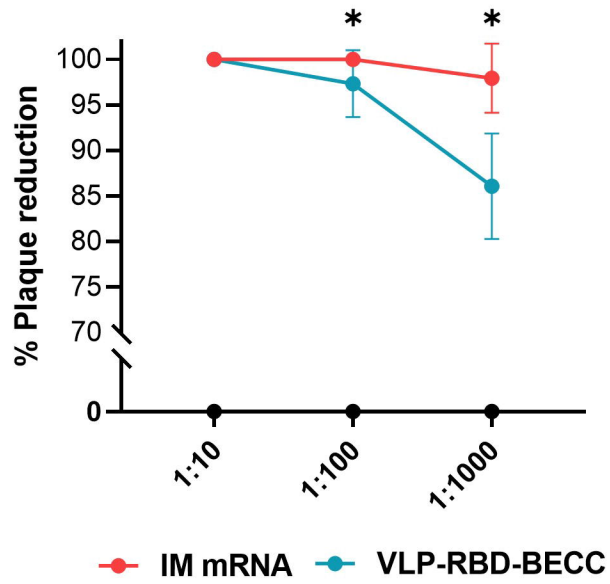
A



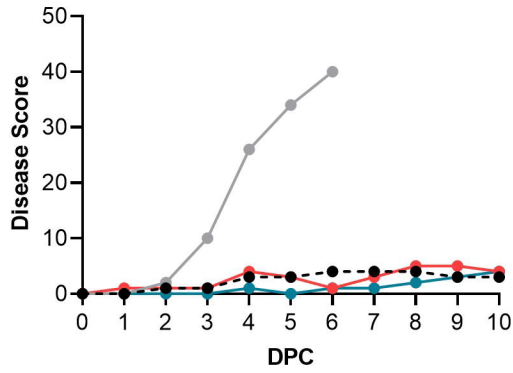
B



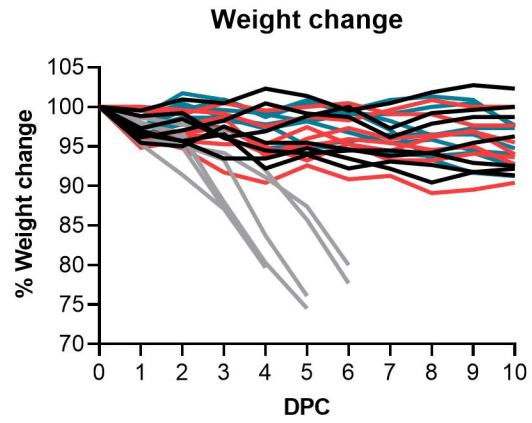
Virus neutralization



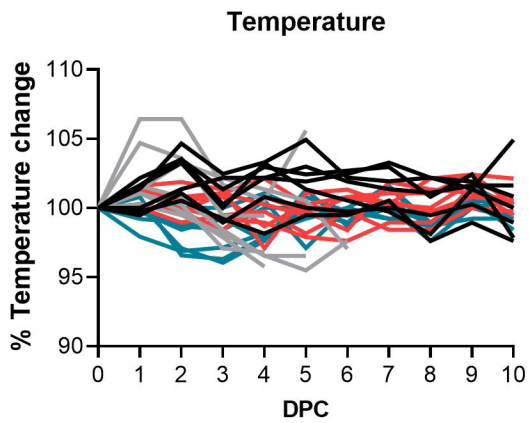
A



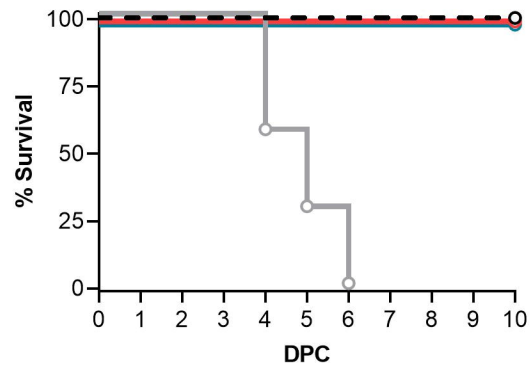
B



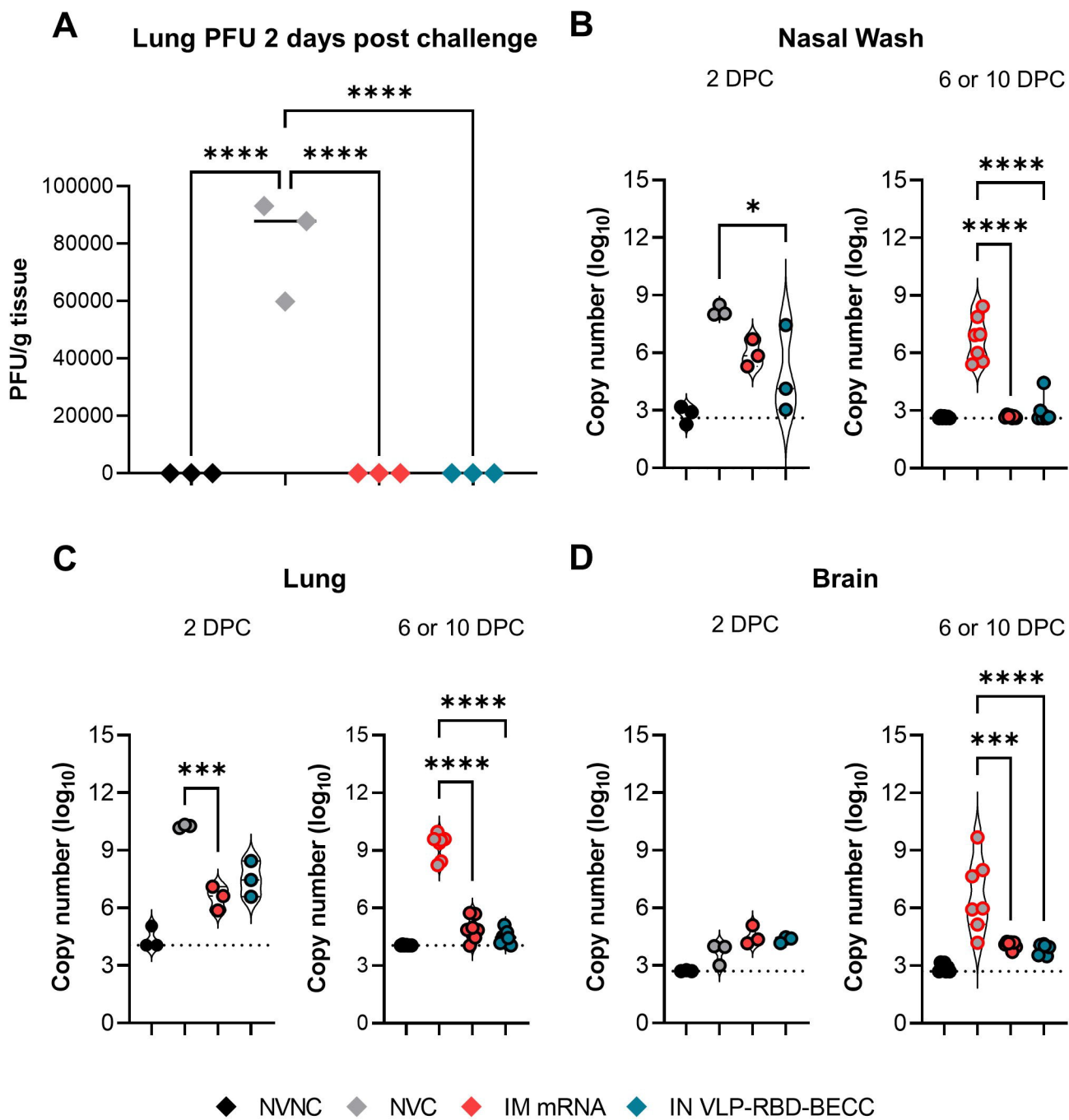
C

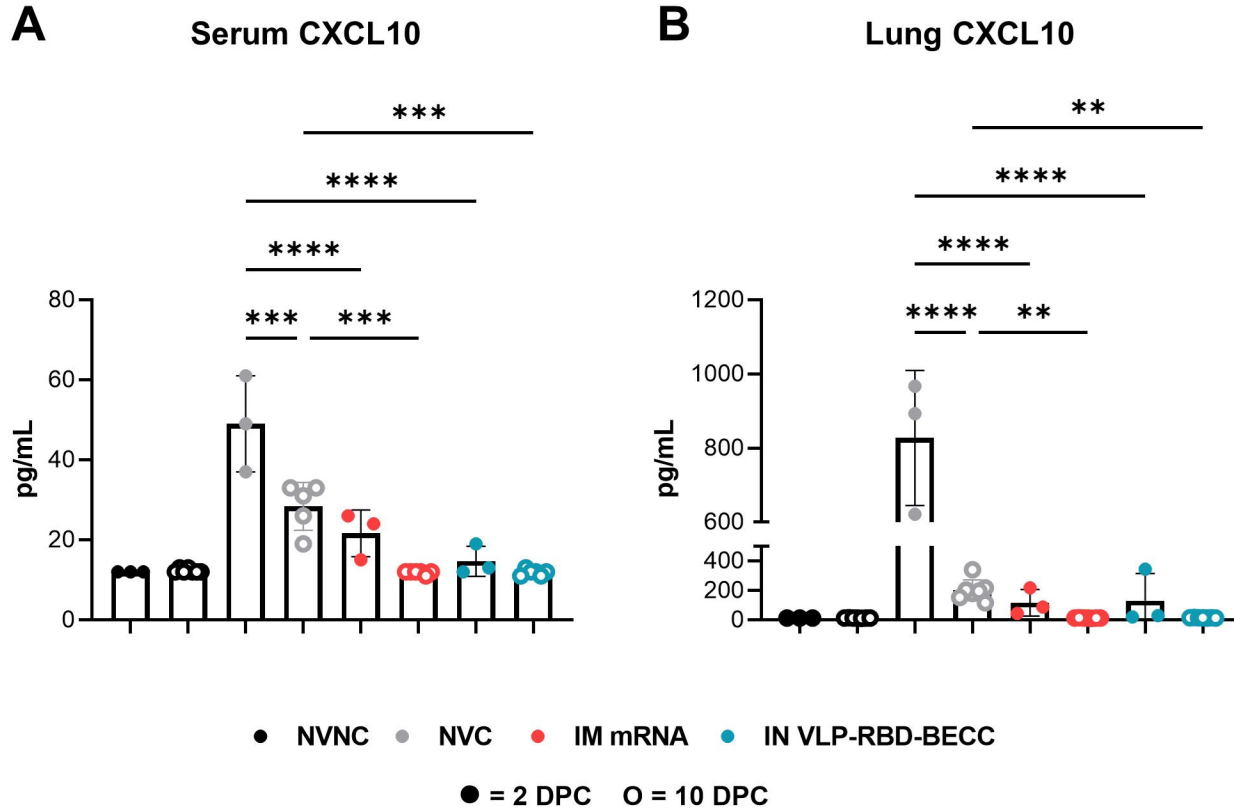


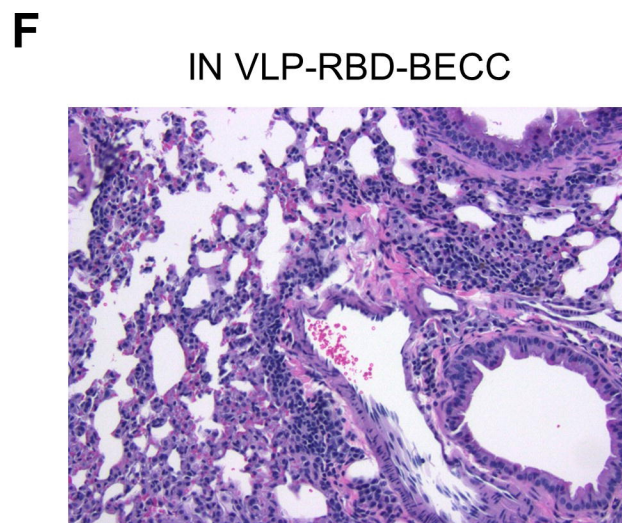
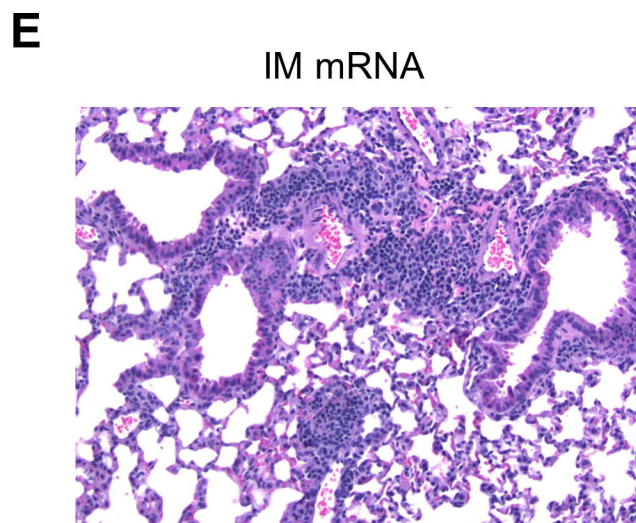
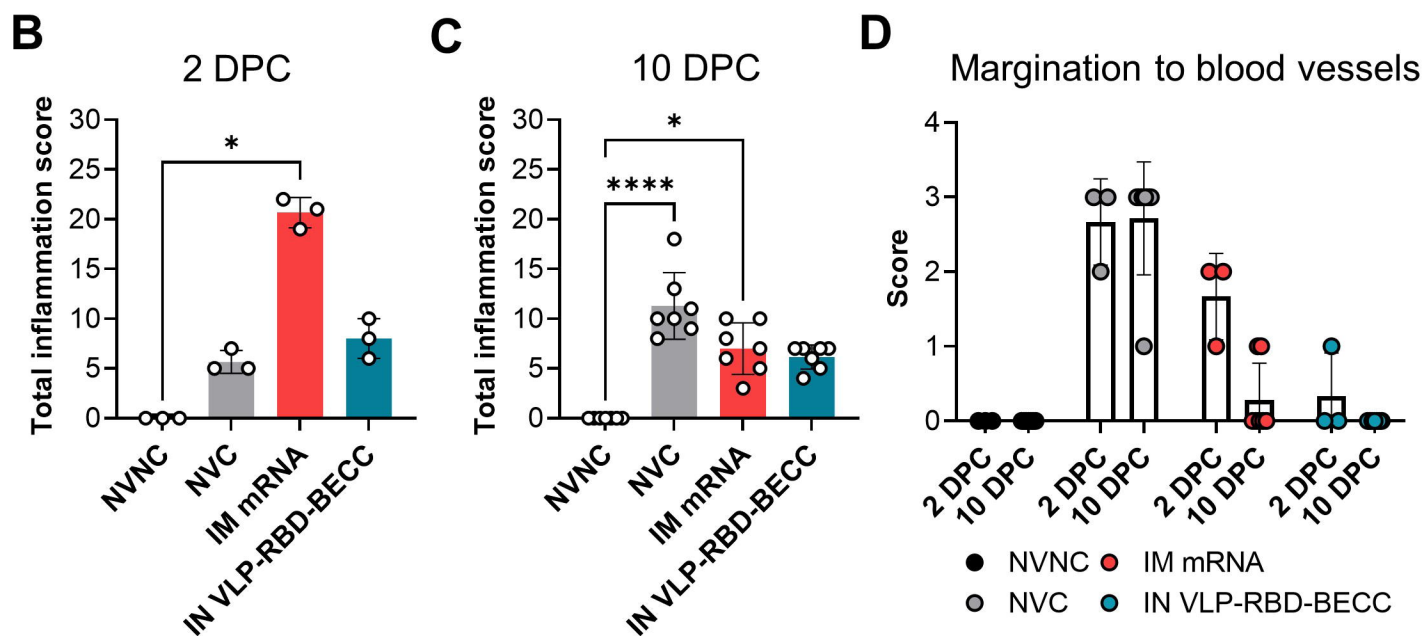
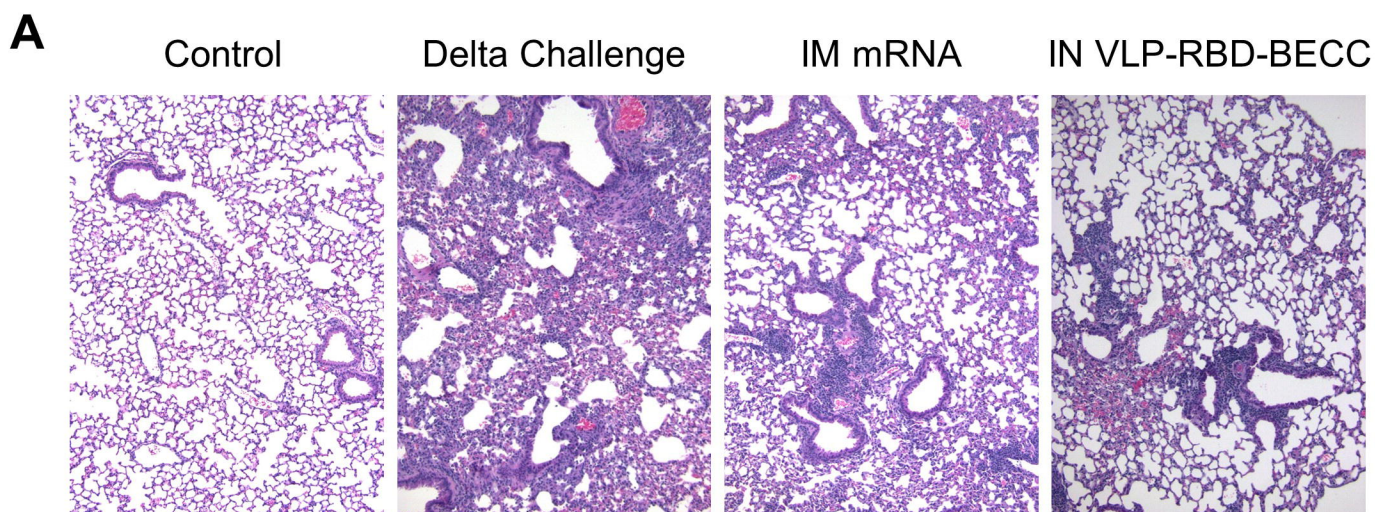
D



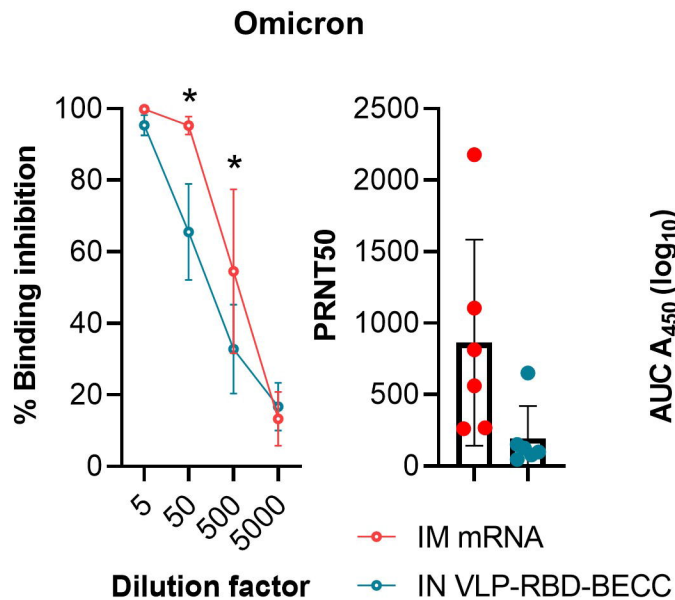
— NVNC — NVC — IM mRNA — IN VLP-RBD-BECC



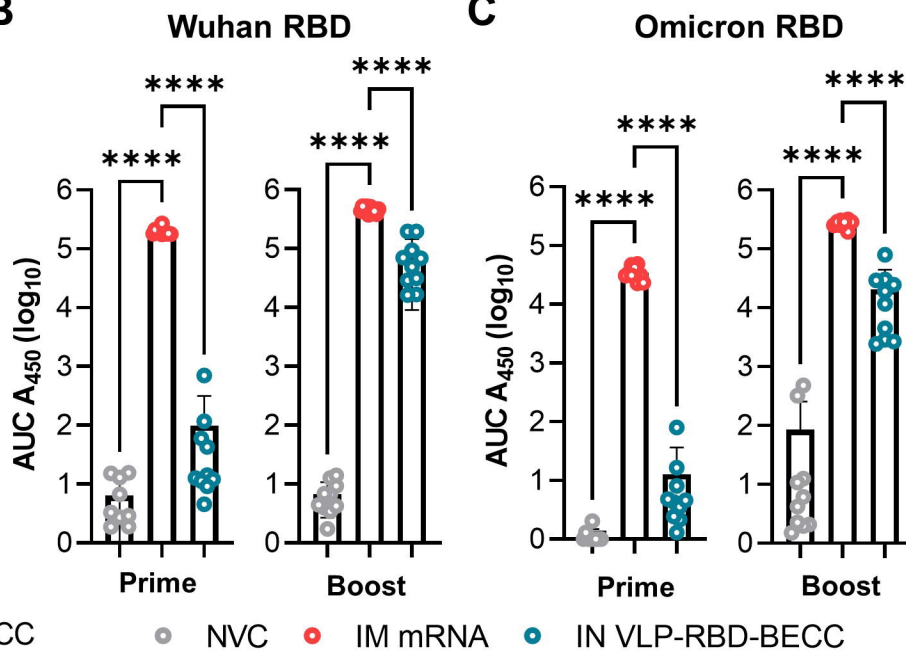




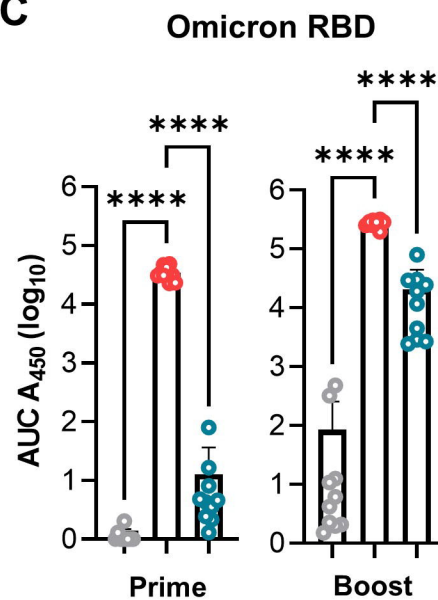
A



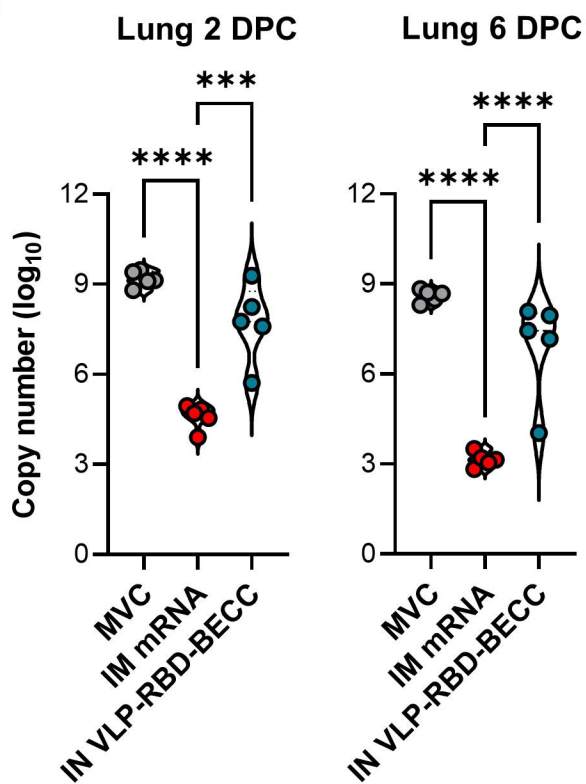
B



C



D



E

